INCORPORATION OF BIO BASED FLAX FIBER REINFORCED POLYMER SKINS FOR PACKAGING ENHANCEMENTS

by

Sufia Sukhyani

A Thesis

Submitted to the Faculty of Purdue University

In Partial Fulfillment of the Requirements for the degree of

Master of Science in Mechanical Engineering

Department of Mechanical and Energy Engineering

Indianapolis, Indiana

December 2021

THE PURDUE UNIVERSITY GRADUATE SCHOOL
STATEMENT OF COMMITTEE APPROVAL

Dr. Hamid Dalir, Chair

Department of Mechanical and Energy Engineering

Dr. Mangilal Agarwal

Department of Mechanical and Energy Engineering

Dr. Andres Tovar

Department of Mechanical and Energy Engineering

Approved by:

Dr. Jie Chen

To all thesis graduate students

ACKNOWLEDGMENTS

It has been a long ride from the day I came to the United States up until the day I defend my thesis. For all that I successfully achieved through these years here at the university I would like to express my sincere gratitude to my advisor Dr. Hamid Dalir for his patience, motivation and guidance throughout these years. His knowledge, wisdom and unequivocal support has been a a driving force in achieving all my goals irrespective of the failures I have faced. I would also like to thank Professor Andres Tovar for providing me the support to score an internship opportunity with Cummins Inc. I am grateful for the support provided by Professor Mangilal Agarwal and Professor Andres Tovar during my time here at the university, sharing their thoughts and feedback which helped me broaden my perspective of research work and for serving as part of my advisory committee.

I would like to thank IUPUI and the entire staff of the Department of Mechanical and Energy Engineering for providing support and assistance during the various stages of my research and internship. I would like to express my gratitude to Linda Wright, Monica Stahlthut, Susan James and Jerry Mooney for their constant guidance and support not only to me but to all those graduate students out there that need them through the years of their master's degree. I would like to acknowledge Randy Newbrough, Anusha Rao, Andi Strackeljahn and the entire crew at the Center of Teaching and Learning for being a constant support the past two years.I would like to thank Benjamin Yeh (mentor)and Kevin Brittain (manager) for their consistent support,guidance and knowledge throughout my internship which has helped me complete most of my tasks within my thesis.

While I make sure I express my gratitude , I cannot forget to acknowledge my Mother/Best Friend Zohra Sukhyani for growing me into a strong independent women like her and my little sister Sufina Sukhyani for being my constant inspiration throughout. A shout out to my extended family Deepak Oswal, Suraj Patil, Azeem Kagadi, Viraj Pisal, Nikhil Patil,Rohan Wani, Neha Barde, Sayali Darne, Pikasa Bagachi and Tejas Magdum for believing in me and my dreams.A toast of gratitude to my family in the states John Joe, Souparna Satipati, Rashmi Menon, Rachana Solanki, Naveen Venugopal who put up with my stupid mistakes. Cheers to the unexpected friendships with Harshal Dhamade, Apurva Desai,Somesh Rath,

Shamika Pujari, Chintan Patel and Sankalp Swami who have been a constant emotional support this year. My last but the best holler goes out to my soulmate Meghana Kamble for being there every single moment making sure I be the best version of myself with a cup of coffee in my hand.

TABLE OF CONTENTS

LIST OF TABLES

LIST OF FIGURES

LIST OF SYMBOLS

σ	stress
ε	strain
τ	shear stress
γ	Shear strain
E	Young's Modulus
ν	poisson's ratio
Q	reduced stiffness
θ	fiber angle
T	Transformation matrix
A_{i_j}	Extensional Stiffness
B_{i_j}	Bending Stiffness
D_{i_j}	Buckling Stiffnes
z_k	laminate thickness
κ	mid-plane curvature
R	radius of corrugation
L	length of corrugation
π	pi
t	thickness
G	shear modulus
ρ	density

ABBREVIATIONS

FRP	Fiber Reinforced Polymer
FEM	Finite Element Modelling
ECT	Edge Crush Test
FCT	Flat Crush test
MPA	Mega Pascal
GPa	Giga Pascal

ABSTRACT

Packaging is a process to wrap goods or products to protect them during transportation and save costs. Transport packages are required to be strong and lightweight in order to be cost effective. Corrugated cardboard is therefore used as it has all these above mentioned features along with it being recyclable.

However, using corrugated cardboard boxes has its own flaws when packing heavy items and storing them due to their low endurance to mechanical stresses. This paper presents an alternative option to corrugated cardboard boxes. Unidirectional flax fabric and bio based epoxy is used to fabricate flax fiber reinforced polymer(FRP) skin which replaced the cardboard skin in corrugated cardboard boxes thus creating a composite sandwich with flax fiber reinforced skin and corrugated cardboard core. Two flute varieties of corrugated cardboard viz. B and C flutes with bulk densities 170 and 127 $\frac{kg}{m^3}$ were used for the core. The complex shaped core is represented by an orthotropic homogenous layer to perform efficient finite element analysis. The orthotropic homogenous layer is validated to have equivalent material properties as that of the corrugated cardboard. As cardboard boxes mainly undergo compressive stress due to stacking one on top of the other, two important tests are carried out to verify the quality of the boxes. These tests are performed using Finite Element Analysis in ANSYS software. Edgewise crush test is carried out to measure the in plane compression stress and Flat crush test is performed to measure the out of plane compression stress. Comparative study between corrugated cardboard boxes and the corrugated cardboard core sandwich boxes with flax fiber reinforced polymer skins via the load vs deformation plot is done to conclude whether the latter is an alternative option in the transportation industry.

Further investigation is done by performing a four point bending test using Finite Element Analysis in ANSYS to understand the flexural deflection for both specimens to provide a better conclusion. Four point bending test is also performed on a specific specimen with dimensions to justify the response of the finite element model with respect to the actual response of the specimen via experimental analysis performed on the specimen.

Keywords: FEM, finite element analysis, corrugated, composite, bio based, Flax, Edge Crush test, Flat crush test, orthotropic, strength, stiffness

1. INTRODUCTION

1.1 Background

Corrugated cardboard boxes are used for packaging goods and storing them in warehouses or transporting them from one destination to another. The most important loading case for storage of these boxes is compressive loading due to the boxes being stacked one upon the other.[1] The other loading case is impact of forklifts during transportation of boxes which lead to indentation in cardboard material causing failure. Compressive loading leads to local buckling due to boxes stacked above them.

Due to wide use of corrugated cardboard boxes in the packaging industry, there is a need of introducing green materials with higher stiffness to avoid failures like local buckling or indentation within the range of compressive loading applied. In order to conclude the material to be introduced, finite element analysis is performed on corrugated cardboard boxes as well as corrugated cardboard core sandwich with flax FRP skins to compare the strength and stiffness in both materials. The Finite Element Analysis performed is justified if there is at least one actual response of the specimen in agreement to the virtual response of the model.

1.2 Aim & Scope of Thesis

The aim of this thesis is to conclude flax FRP skins with corrugated cardboard core as an alternative solution to corrugated cardboard boxes in the packaging industry. Two types of standard corrugated cardboard flutes are modelled viz. B and C flutes. The corrugated cardboard is made of three different parts, two being the liners and the middle part being the core placed between the liners. The liners are made of cardboard in standard cardboard boxes and the core is made of corrugated cardboard. As an alternative solution, the liners are replaced by flax fiber reinforced skins bound together with a bio based epoxy **sad18**. The corrugated cardboard geometry is complex as it would require a high number of elements and more computational time during the simulation. In order to simplify the process, the complex geometry is represented by a homogeneous orthotropic plate with equivalent mate-

rial properties calculated via an analytical method. **7**, [2]–[4] As the most important loading case for the boxes are compressive stresses, two major test are carried out on both specimens for both flute varieties. Edgewise crush test measures the in plane compressive strength and flat crush test measures the out of plane compressive strength of both specimens. Comparative study is carried out to conclude the whether the corrugated core sandwich with flax FRP skins as an alternative solution via the load vs displacement plots for both tests using finite element analysis in Ansys. Finite Element Analysis performed is justified if there is at least an actual response of the specimen in agreement to the virtual response of the model. Therefore, a four point bending analysis is performed on the specimen to validate the experimental analysis in reference (3) Corrugated Cardboard Core Sandwich Beams with Bio-based Flax Fiber Composite Skins.

1.3 Formulation of the Problem

Introducing an alternative solution to corrugated cardboard requires a comparative study of both specimens viz. corrugated cardboard and corrugated cardboard core sandwich with Flax FRP skins. The comparative study involves comparison between strength and stiffness of both specimens with the help of load vs displacement plot obtained from the edgewise crush test and flat crust test which replicate the most important loading case of the corrugated boxes.

1.4 Procedure of Solving the Problem

Computer Aided Design modelling software SOLIDWORKS and Finite Element Analysis software Ansys are used in the process of modelling and simulating the various tests to conclude the results for the thesis. Step by Step procedure of the work done is mentioned below. enumitem

- Create a detailed model of B and C flute in Computer Aided Design software SOLIDWORKS

- Calculate the equivalent orthotropic material properties for a homogenized model of the complex corrugated geometry for both specimens.
- Validate the equivalent material properties of the homogenized model by performing Finite Element Analysis in Ansys for both specimens by measuring the displacement.
- Perform Edgewise crush test on both specimens for both flutes to plot load vs displacement graph.
- Compare the load vs displacement graph for both specimens for both flutes.
- Perform Flat crush test on both specimens for both flutes to plot load vs displacement graph.
- Compare the load vs displacement graph for both specimens for both flutes.
- Perform four point bending test on both specimens for both flutes to understand the flexural stiffness.
- Perform four point bending test with similar dimensions of the specimen mentioned in reference paper 3 to justify the virtual response of the model to the actual response obtained from the experimental analysis mentioned in the paper.
- Derive a conclusion about using Corrugated cardboard core sandwich boxes with Flax FRP skins as an alternative solution to the transportation industry.

2. CORRUGATED CARDBOARD

2.1 History

Wooden crates were used earlier as a mean for moving materials before the cardboard box was even invented. In 1856, corrugated paper was used as a liner in hats. It was not until 1871 that corrugated cardboard boxes were used for shipping and handling. The improvement of the machines made it possible to produce the corrugated board of higher quality. In 1920's boxes made of corrugated board started to compete with the ones made of wood. [1], [5]

2.2 Manufacturing

Corrugated cardboard layers are assembled by gluing together cardboard paper and cardboard core. The cardboard paper are called liners and the corrugated cardboard placed in between the liners is called the core.

The manufacturing process of corrugated cardboard can be done in two different ways. One of the ways is called the wet part where the fluting is corrugated between two rolls and then glued on the liner. The other process is termed as the dry part where heat is applied to dry the corrugated board and push it on to the liner. [1]

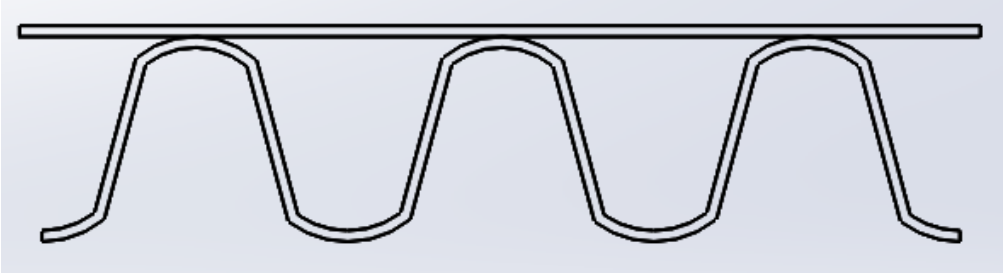

Figure 2.1. Different types of corrugated cardboard
a) Single face

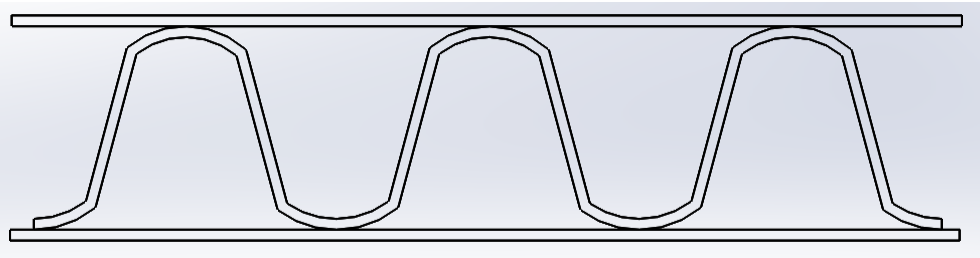

Figure 2.2. Different types of corrugated cardboard
b) Single wall

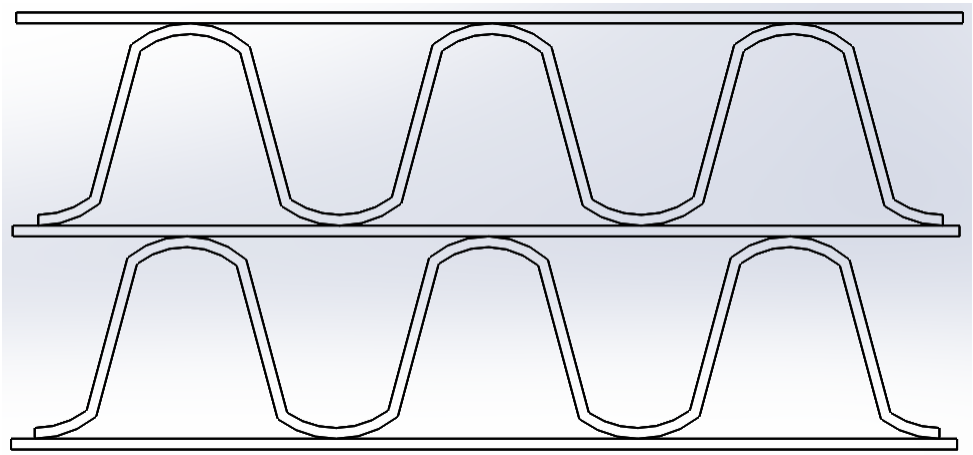

Figure 2.3. Different types of corrugated cardboard
c) Double wall

A problem in manufacturing of corrugated cardboard is the moisture content. If the moisture content is out of balance, it results in deformation in terms of buckling. This phenomena caused is called warp or washboard.

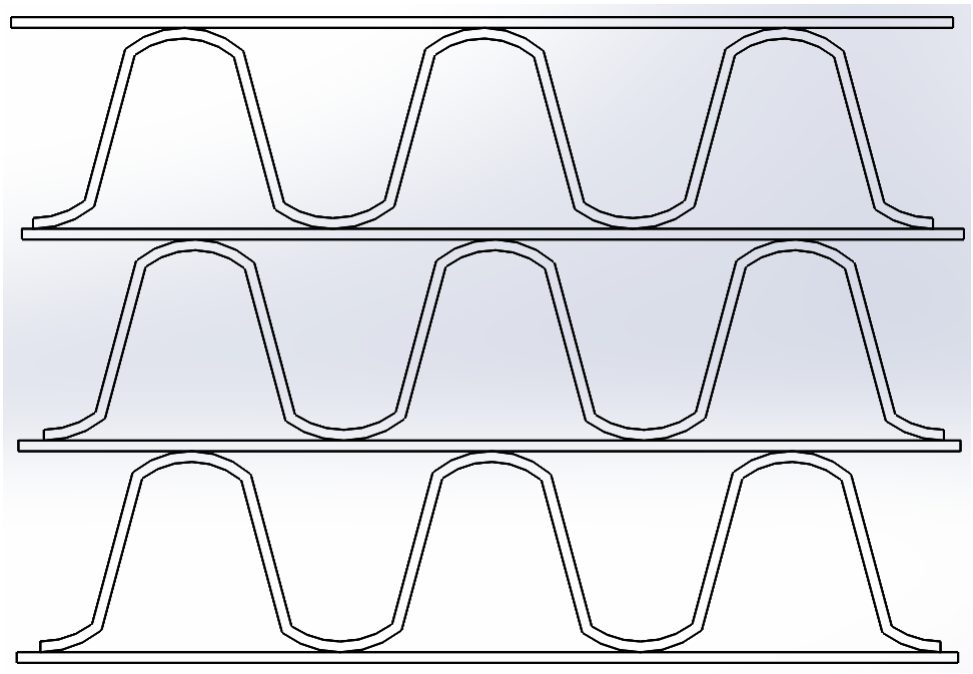

Figure 2.4. Different types of corrugated cardboard
d) Triple wall

Cardboard is an orthotropic material ,therefore, it has different materials properties in different planes. The different planes are determined as follows.

There are different types of flute profiles as well used for different applications.

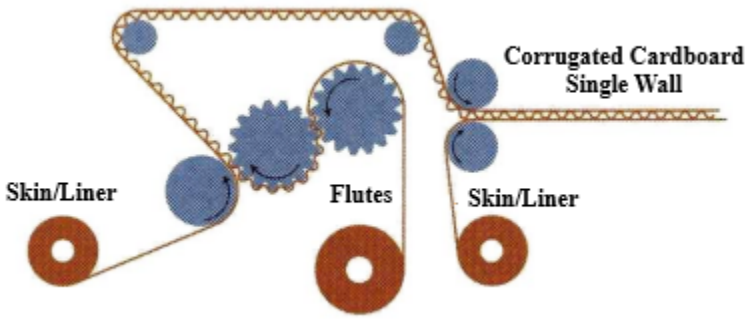

Figure 2.5. Manufacturing of single wall of corrugated cardboard [1]

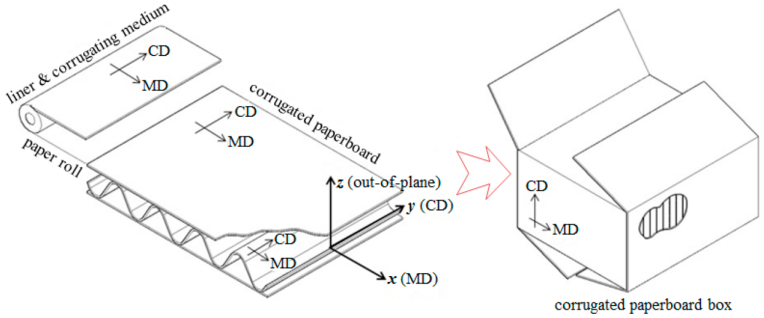

Figure 2.6. Orthotropic properties of corrugated cardboard defining fiber direction And flute direction [6]

2.3 Applications

Corrugated cardboard boxes are used mainly for packaging. Advantage of using corrugated cardboard is that it can be customized for different purposes. The low weight helps in saving money during transportation. The strength to weight ratio is high which provides required protection to the goods it carries. The application of corrugation varies depending on the type flute. Higher value of thickness provides more cushioning to the goods thus using such flutes for delicate goods whereas lower value of thickness is great for retail and mailing purposes. Corrugated cardboard is easy to handle, print as well as recycle. However, corru-

Table 2.1. Different types of flute and its applications [6]

Flute Profile	Number of Flutes/foot	Thickness (mm)	Application
A	33	4.0	Cushioning for fragile products
B	47	3.2	Canned goods, beverage trays
C	39	4.0	Shipping cases, furniture
E	90	1.6	Small retail packaging
F	125	0.8	Small retail packaging

gated cardboard has its own disadvantages. Corrugated cardboard undergoes compressive loading as its most important loading during stacking boxes in warehouses. This results in compressive loading of boxes by the boxes stacked right on top. The flaw in such boxes is that it undergoes local buckling or deformation due to its application.

3. THEORY

This chapter describes the theory of methodology being used in the further chapter. It will give you a basic understanding of each concept based on which the further analysis is carried out.

3.1 Corrugated Cardboard

Two types of corrugated cardboard flute types are considered in this thesis. B flute is one of the types of flutes used for supporting heavier items. C flute is commonly used for shipping and provides better cushioning than B flute. These flutes are taken into consideration as they involve the application of transporting heavier items thus resulting in more compressive load when stacked one upon the other.

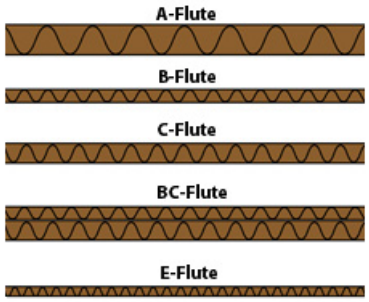

Figure 3.1. Single wall flutes [7]

The corrugated cardboard consists of two different parts put together. There are two facings called as the liners and there is a corrugated core placed between these liners called as the fluting or the flute. The purpose of the corrugated core is to provide stability to the facings by resisting shear stresses. The corrugated core has high stiffness and strength due to its geometry. It provides sufficient rigidity to forces perpendicular to it thus cushioning the products placed inside the box. The liners are placed on either ends of the core to provide resistance to the compressive stresses along the axis. When the liner and core are placed individually they have no stability or rigidity at all. However, When they are placed together

they form a high strength to weight ratio material which can resist both compressive stresses as well as shear stresses to fulfill the objective of cushioning the products it holds. [1].

3.2 Composite Sandwich Structure

Composite sandwich structures with Flax fiber reinforced polymer skins used as the liner and corrugated cardboard as the core is proposed as an alternative solution to cardboard boxes. Flax fiber reinforced polymer skins are light in weight and provide an increase in strength and stiffness as compared to just cardboard skins. Fiber reinforced skins are expected to provide resistance to compressive stresses along the axis as well as flexural stress. The corrugated cardboard core is still expected to resist shear stresses [1], [8]–[10].

Fiber reinforced polymer composites are mainly made of synthetic fibers such as grass or carbon fibers. These fiber reinforced polymers are used as skins for composite panels in many applications, however, plant based natural fibers are being explored for other applications. One of the applications are using Flax fiber reinforced skins with corrugated cardboard cores in the form of wall, cladding roof and floor panels to improve structural efficiency and insulation properties. Along with flax, hemp is also a natural fiber that is being explored for various applications.[1], [8]–[10] Synthetic fiber reinforced polymers have higher strength than the natural fibers however, using synthetic fiber doesn't provide an eco-friendly and environment conscious alternative which is a mandatory requirement in today's age. Natural fibers have that advantage of being environmentally safe as compared to its synthetic counterparts while providing viable structural rigidity required for the application. In fiber reinforced polymers, polymer resins used to bond the fibers are also synthetic. Epoxy and vinyl ester are commonly used with natural fibers as well. Although, multiple studies have been done with the resins being partially and fully bio based while bonding natural fibers. [11]–[15]. SUPER SAP ONE is a bio based epoxy which contains 30% bio content to bind the flax fibers when fabricating the fiber reinforced polymer skins in this paper [1].

Different core materials are also being explored to provide structural support in sandwich structures. Foam, plastic or metal honeycombs are commonly studied as core materials due to their low density. Foam is the most used core during manufacture of many synthetic composites. In this paper, however, taking into consideration the cost of manufacturing the cardboard boxes, corrugated cardboard has been the cheapest and easy to manufacture material which can be used. Due to its corrugation geometry, it's still provide the structural rigidity required to resist the shear stresses while being eco-friendly and environmentally safe as compared to other core options. It fulfills the objectives of providing high load carrying capacity with low weight. Corrugated cardboard core with flax fiber reinforced skins as composite sandwich have only been studied on in the construction industry as sandwich beams for walls, cladding, roof and floor panels to improve structural efficiency and insulation properties.

In this paper, improvement in structural efficiency is required while maintaining insulation properties and therefore this composite sandwich is an alternative that can be proposed to corrugated boxes if it improves resistance to compressive stresses in plane and out of plane. The corrugated cardboard core of two different flute varieties (B & C) are being considered. The unidirectional flax fiber reinforced skins are bound together using a bio based epoxy Super Sap One with 30% bio content. Thus, a green composite sandwich structure is analyzed and compared to the corrugated cardboard box to be proposed as an alternative solution to avoid minimal flaws cardboard boxes have.

3.3 Evaluation of Equivalent Stiffness Properties of Corrugated Cardboard

Corrugation is described as a series of parallel ridges or furrows. Most famous patterns used for corrugation are round corrugation and trapezoidal corrugation.

In cardboard boxes, round corrugation is the standard corrugation used. There are varieties of round corrugation depending on the height of the flute. The five most standard flute profiles are A, B, C, E F. Corrugation is the most important feature of corrugated cardboard as it provides structural stability with limited thickness. Due to small thickness and complex geometry, it becomes a tedious job to model and mesh the geometry as it

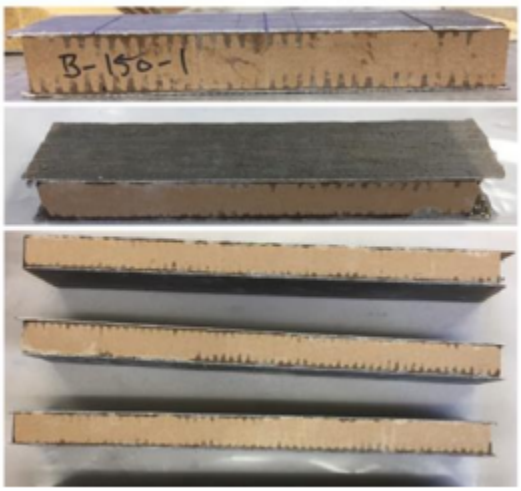

Figure 3.2. Corrugated cardboard core sandwich beams with bio based Flax Fiber reinforced composite skins [7]

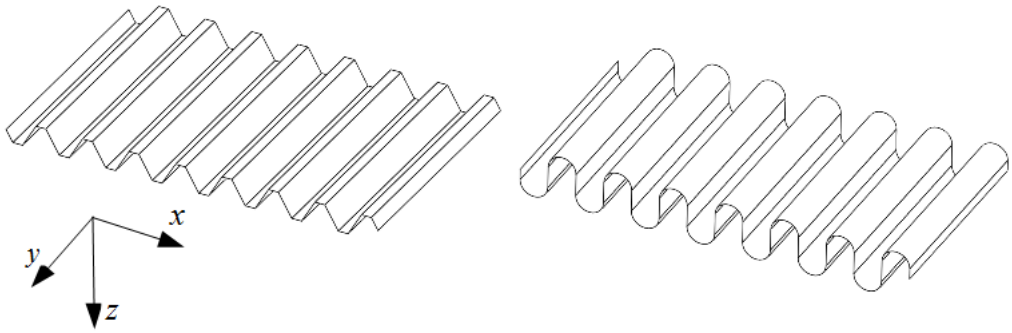

Figure 3.3. Corrugated cardboard core sandwich beams with bio based Flax Fiber reinforced composite skins [15]

requires high number of elements while adding computational time. In order to limit the number of elements and reduce computational time, a homogenous orthotropic plate with same dimensions and thickness as that of the corrugation is modelled. As the thickness of the homogenous orthotropic plate is kept similar, the stiffness and equivalent mechanical properties of the homogenous layer are calculated using an analytical method. **7**, [3], [4]

As cardboard is an orthotropic material it has material properties in three different directions. According to the classical laminated plate theory for orthotropic materials, The stress – strain relationship can be expressed as:

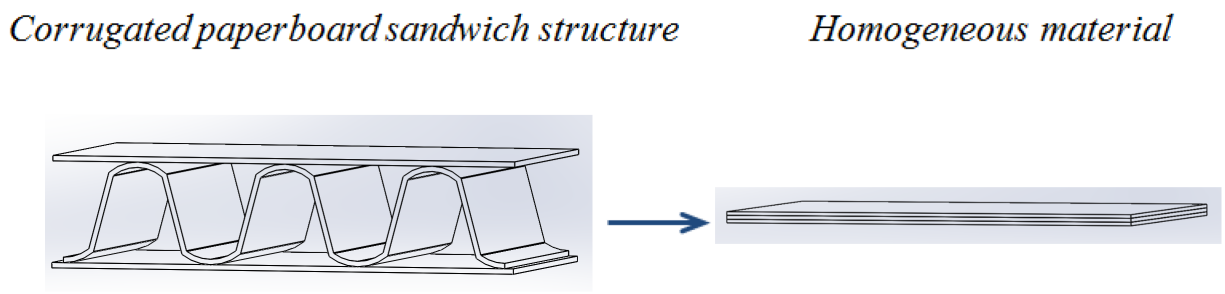

Figure 3.4. Corrugated Model to Simplified model with equivalent properties [7]

$$\begin{Bmatrix} \sigma_1 \\ \sigma_2 \\ \tau_{12} \end{Bmatrix} = \begin{bmatrix} Q_{11} & Q_{12} & 0 \\ Q_{12} & Q_{22} & 0 \\ 0 & 0 & Q_{66} \end{bmatrix} \begin{Bmatrix} \varepsilon_1 \\ \varepsilon_2 \\ \gamma_{12} \end{Bmatrix} [16] \tag{3.1}$$

where, [Q] is the reduced stiffness matrix. It can be calculated as below;

$$Q_{11} = \frac{E_1}{1 - \nu_{12}\nu_{21}} [16] \tag{3.2}$$

$$Q_{22} = \frac{E_2}{1 - \nu_{12}\nu_{21}} [16] \tag{3.3}$$

$$Q_{12} = \frac{\nu_{21}E_2}{1 - \nu_{12}\nu_{21}} [16] \tag{3.4}$$

$$Q_{66} = G_{12} [16] \tag{3.5}$$

The fiber direction can be placed at different angles. The most common angles are $0°, 30°, 45°, \& \ 90°$.

For achieving the reduced stiffness matrix in any other direction, we use a transformation matrix;

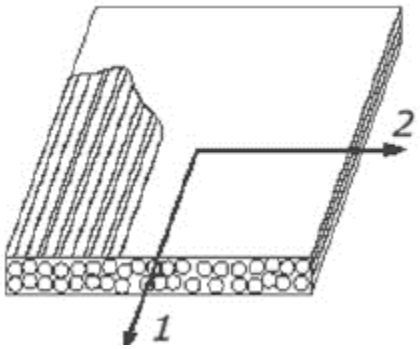

Figure 3.5. Fiber direction and transverse direction in composite matrix [16]

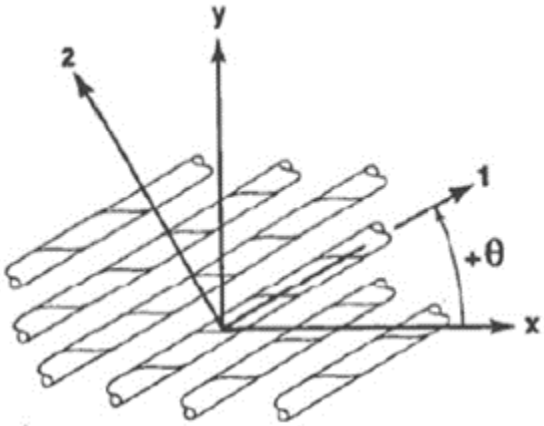

Figure 3.6. Global coordinate for matrix and local coordinate for fibers [16]

$$[T] = \begin{bmatrix} cos^2\theta & sin^2\theta & 2sin\theta cos\theta \\ sin^2\theta & cos^2\theta & -2sin\theta cos\theta \\ -sin\theta cos\theta & sin\theta cos\theta & cos^2\theta - sin^2\theta \end{bmatrix} [16] \tag{3.6}$$

To obtain the transformed stiffness matrix

$$[\bar{Q}] = [T^{-1}][Q][T^{-T}][16] \tag{3.7}$$

$$Q_{\bar{1}\bar{1}} = Q_{11}cos^4\theta + 2(Q_{12} + 2Q_{66})sin^2\theta cos^2\theta + Q_{22}sin^4\theta \tag{3.8}$$

$$Q_{\bar{1}\bar{2}} = (Q_{11} + Q_{22} - 4Q_{66})sin^2\theta cos^2\theta + Q_{12}(sin^4\theta + cos^4\theta) \tag{3.9}$$

$$Q_{\bar{2}\bar{2}} = Q_{11}sin^4\theta + 2(Q_{12} + 2Q_{66})sin^2\theta cos^2\theta + Q_{22}cos^4\theta \tag{3.10}$$

$$Q_{\bar{1}\bar{6}} = (Q_{11} - Q_{12} - 2Q_{66})sin\theta cos^3\theta + (Q_{12} - Q_{22} + 2Q_{66})sin^3\theta cos\theta \tag{3.11}$$

$$Q_{\bar{2}\bar{6}} = (Q_{11} - Q_{12} - 2Q_{66})sin^3\theta cos\theta + (Q_{12} - Q_{22} + 2Q_{66})sin\theta cos^3\theta \tag{3.12}$$

$$Q_{\bar{6}\bar{6}} = (Q_{11} + Q_{22} - 2Q_{12} - 2Q_{66})sin^2\theta cos^2\theta + Q_{66}(sin^4\theta + cos^4\theta) \tag{3.13}$$

The transformed stress strain relationship becomes:

$$\begin{Bmatrix} \sigma_x \\ \sigma_y \\ \tau_{xy} \end{Bmatrix} = \begin{bmatrix} Q_{\bar{1}\bar{1}} & Q_{\bar{1}\bar{2}} & 0 \\ Q_{\bar{1}\bar{2}} & Q_{\bar{2}\bar{2}} & 0 \\ 0 & 0 & Q_{\bar{6}\bar{6}} \end{bmatrix} \begin{Bmatrix} \varepsilon_x \\ \varepsilon_y \\ \upsilon_{xy} \end{Bmatrix} \tag{3.14}$$

[16]

Using the transformed stiffness matrix, the extensional, coupling and bending stiffness matrix can be calculated. Together the stiffness matrix is called the ABD matrix.

The extensional stiffness matrix can be calculated using the following formula

$$A_{\mathrm{ij}} = \sum_{k=1}^{N} (Q_{\bar{\mathrm{ij}}})_k (z_k - z_{k-1}) \tag{3.15}$$

[16]

The coupling stiffness matrix is calculated using the formula below

$$B_{\mathrm{ij}} = \frac{1}{2} \sum_{k=1}^{N} (Q_{\bar{\mathrm{ij}}})_k (z_k^2 - Z_{k-1}^2) \tag{3.16}$$

[16]

Coupling stiffness matrix will be equal to zero if the laminate has symmetric lay up respect to the middle surface.

The bending stiffness matrix is calculated using the formula below.

$$D_{\mathrm{ij}} = \frac{1}{3}\sum_{k=1}^{N} Q_{\bar{\mathrm{ij}}k}(Z_k^3 - Z_{k-1}^3) \tag{3.17}$$

[16]

The ABD matrix becomes

$$\left[\begin{array}{ccc|ccc} A_{11} & A_{12} & A_{16} & B_{11} & B_{12} & B_{16} \\ A_{12} & A_{22} & A_{26} & B_{12} & B_{22} & B_{26} \\ A_{16} & A_{26} & A_{66} & B_{16} & B_{26} & B_{66} \\ \hline B_{11} & B_{12} & B_{16} & D_{11} & D_{12} & D_{16} \\ B_{12} & B_{22} & B_{26} & D_{12} & D_{22} & D_{26} \\ B_{16} & B_{26} & B_{66} & D_{16} & D_{26} & D_{66} \end{array}\right]$$

Resultant forces in the laminated thin plate can be calculated as

$$\begin{Bmatrix} N_x \\ N_y \\ N_{xy} \end{Bmatrix} = \begin{bmatrix} A_{11} & A_{12} & A_{16} \\ A_{12} & A_{22} & A_{26} \\ A_{16} & A_{26} & A_{66} \end{bmatrix} \begin{Bmatrix} \varepsilon_x^0 \\ \varepsilon_y^0 \\ \upsilon_{xy}^0 \end{Bmatrix} + \begin{bmatrix} B_{11} & B_{12} & B_{16} \\ B_{12} & B_{22} & B_{26} \\ B_{16} & B_{26} & B_{66} \end{bmatrix} \begin{Bmatrix} \kappa_x \\ \kappa_y \\ \kappa_{xy} \end{Bmatrix} \tag{3.18}$$

where $\begin{Bmatrix} \kappa_x \\ \kappa_y \\ \kappa_{xy} \end{Bmatrix}$ represent the middle surface curvatures.

Resultants moments can be calculated as

$$\begin{Bmatrix} M_x \\ M_y \\ M_{xy} \end{Bmatrix} = \begin{bmatrix} B_{11} & B_{12} & B_{16} \\ B_{12} & B_{22} & B_{26} \\ B_{16} & B_{26} & B_{66} \end{bmatrix} \begin{Bmatrix} \varepsilon_x^0 \\ \varepsilon_y^0 \\ \Upsilon_{xy}^0 \end{Bmatrix} + \begin{bmatrix} D_{11} & D_{12} & D_{16} \\ D_{12} & D_{22} & D_{26} \\ D_{16} & D_{26} & D_{66} \end{bmatrix} \begin{Bmatrix} \kappa_x \\ \kappa_y \\ \kappa_{xy} \end{Bmatrix} \tag{3.19}$$

The corrugated panel is repeated by a sinusoidal wave. Therefore, to calculate stiffness properties a basic unit cell or unit profile is used. This is termed as Representative Volume Element (RVE). The sinusoidal wave is representated in local curvilinear coordinates (s,n,y).

Resultant Forces and Moments can be calculated as follows:

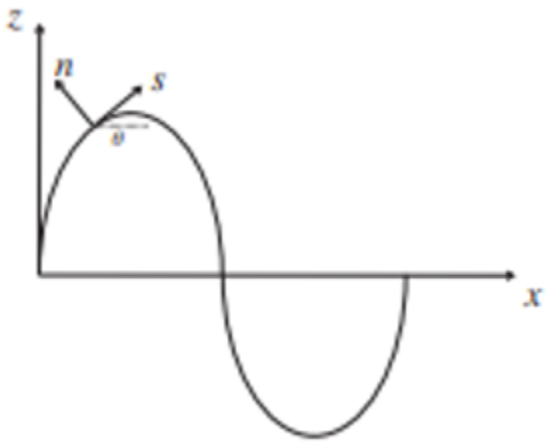

Figure 3.7. Round Corrugation [17]

$$\begin{Bmatrix} N_s \\ N_y \\ N_{sy} \\ M_s \\ M_y \\ M_{sy} \end{Bmatrix} = \begin{bmatrix} A_{11} & A_{12} & A_{16} & 0 & 0 & 0 \\ A_{12} & A_{22} & A_{26} & 0 & 0 & 0 \\ A_{16} & A_{26} & A_{66} & 0 & 0 & 0 \\ 0 & 0 & 0 & D_{11} & D_{12} & D_{16} \\ 0 & 0 & 0 & D_{12} & D_{22} & D_{26} \\ 0 & 0 & 0 & D_{16} & D_{26} & D_{66} \end{bmatrix} \begin{Bmatrix} \varepsilon_s^0 \\ \varepsilon_y^0 \\ \upsilon_{sy} \\ \kappa_s \\ \kappa_y \\ \kappa_{sy} \end{Bmatrix} \tag{3.20}$$

There are two methods required to calculate the equivalent stiffness of the orthotropic plate model.

The equivalent energy method calculates the strain energy of the corrugated panel which can be done by the following formula

$$U = \frac{1}{2} \int \int N^T S N ds dy$$

[18]

where N = $\begin{Bmatrix} N_s \\ N_y \\ N_{sy} \\ M_s \\ M_y \\ M_{sy} \end{Bmatrix}$ and S is the inverse of the stiffness matrix $\begin{Bmatrix} A & 0 \\ 0 & D \end{Bmatrix}$

$$\begin{bmatrix} S_{11} & S_{12} & 0 & 0 & 0 & 0 \\ S_{12} & S_{22} & 0 & 0 & 0 & 0 \\ 0 & 0 & S_{33} & 0 & 0 & 0 \\ 0 & 0 & 0 & S_{44} & S_{45} & 0 \\ 0 & 0 & 0 & S_{45} & S_{55} & 0 \\ 0 & 0 & 0 & 0 & 0 & S_{66} \end{bmatrix}$$

where,

$$S_{11} = \frac{A_{22}}{A_{11}A_{22} - A_{(12)}^2} \tag{3.22}$$

$$S_{12} = \frac{-A_{12}}{A_{11}A_{22} - A_{(12)}^2}$$

$$S_{22} = \frac{A_{11}}{A_{11}A_{22} - A_{(12)}^2} \tag{3.23}$$

$$S_{33} = \frac{1}{A_{66}}$$

$$S_{44} = \frac{D_{22}}{D_{11}D_{22} - D_{(12)}^2} \tag{3.24}$$

$$S_{45} = \frac{-D_{12}}{D_{11}D_{22} - D_{(12)}^2}$$

$$S_{55} = \frac{D_{11}}{D_{11}D_{22} - D_{(12)}^2} \tag{3.25}$$

$$S_{66} = \frac{1}{D_{66}}$$

The integration is carried out over a period of 2c and width of b.

The equivalent energy method calculates only the diagonal terms. Six generalized boundary conditions are considered to calculate the equivalent stiffness matrices.

$$\begin{Bmatrix}1,0,0,0,0,0\end{Bmatrix}^T$$
$$\begin{Bmatrix}0,1,0,0,0,0\end{Bmatrix}^T$$
$$\begin{Bmatrix}0,0,1,0,0,0\end{Bmatrix}^T$$
$$\begin{Bmatrix}0,0,0,1,0,0\end{Bmatrix}^T$$
$$\begin{Bmatrix}0,0,0,0,1,0\end{Bmatrix}^T$$
$$\begin{Bmatrix}0,0,0,0,0,1\end{Bmatrix}^T$$

For case 1, when

$$\begin{Bmatrix}\varepsilon^-,\kappa^-\end{Bmatrix} = \begin{Bmatrix}1,0,0,0,0,0\end{Bmatrix}^T \tag{3.26}$$

;

Using strain energy equation;

$$U = \frac{1}{2}\int\int_A (N_s^2 S_{11} + 2N_s N_y S_{12} + N_y^2 S_{22} + M_s^2 S_{44} + 2M_s M_y S_{45} + M_y^2 S_{55}) ds dy$$

The stiffness matrix for the equivalent orthotropic plate is in global coordinates (x,y,z). The resultant forces and moments for the equivalent orthotropic plate can be calculated as

$$\begin{Bmatrix} N_x \\ N_y \\ N_{xy} \\ M_x \\ M_y \\ M_{xy} \end{Bmatrix} = \begin{bmatrix} A_{11} & A_{12} & A_{16} & 0 & 0 & 0 \\ A_{12} & A_{22} & A_{26} & 0 & 0 & 0 \\ A_{16} & A_{26} & A_{66} & 0 & 0 & 0 \\ 0 & 0 & 0 & D_{11} & D_{12} & D_{16} \\ 0 & 0 & 0 & D_{12} & D_{22} & D_{26} \\ 0 & 0 & 0 & D_{16} & D_{26} & D_{66} \end{bmatrix} \begin{Bmatrix} \varepsilon_x^0 \\ \varepsilon_y^0 \\ \upsilon_{xy} \\ \kappa_x \\ \kappa_y \\ \kappa_{xy} \end{Bmatrix} \tag{3.28}$$

Now in terms of global coordinates;

$$N_s = N_x(\frac{dx}{ds}) \tag{3.29}$$

,

$$M_s = N_x z \tag{3.30}$$

Using the boundary conditions with zero strain and zero curvature in y direction in local coordinates,

$$N_y = \frac{A_{12}}{A_{11}} \tag{3.31}$$

$$M_y = \frac{D_{12}}{D_{11}} \tag{3.32}$$

Substituting above equations,

$$U = \frac{1}{2}\int_0^b \int_s [N_s^2(\frac{dx}{ds})^2 S_{11} + 2\frac{A_{12}}{A_{11}}S_{12} + \frac{(A_{12})^2}{A_{(11)^2}}S_{22} + N_x^2 z^2 S_{44} + 2N_x z\frac{D_{12}}{D_{11}}S_{45} + \frac{D_{(12)}{}^2}{D_{(11)^2}}S_{55}]dsdy \tag{3.33}$$

$$U = \frac{1}{2}\int_0^b \int_s N_x[(\frac{dx}{ds})^2(S_{11} + 2\frac{A_{12}}{A_{11}}S_{12} + \frac{A_{(12)}{}^2}{A_{(1_1^2)}}S_{22}) + z^2(S_{44} + 2\frac{D_{12}}{D_{11}}S_{45} + \frac{D_{(12)}{}^2}{D_{(11)^2}}S_{55}]dsdy \tag{3.34}$$

$$U = \frac{1}{2}bN_x^2\int_s [(\frac{dx}{ds})^2(S_{11} + 2\frac{A_{12}}{A_{11}}S_{12} + \frac{A_{(12)}{}^2}{A_{(1_1^2)}}S_{22}) + z^2(S_{44} + 2\frac{D_{12}}{D_{11}}S_{45} + \frac{D_{(12)}{}^2}{D_{(11)^2}}S_{55}]ds \tag{3.35}$$

Substituting values for $S_{11}.S_{12}, S_{22}, S_{44}, S_{45}, S_{55}$;

we get,

$$U = \frac{1}{2} b N_x^2 \int_s [(\frac{dx}{ds})^2 \frac{1}{A_{11}} + z^2 \frac{1}{D_{11}}] ds \tag{3.36}$$

$$U = \frac{1}{2} b N_x^2 [\frac{I_1}{A_{11}} + \frac{I_2}{D_{11}}] \tag{3.37}$$

where, $I_1 = \int_s (\frac{dx}{ds})^2$ $I_2 = \int_s z^2 ds$

Now using boundary conditions for strain in global coordinates

$N_x^- = A_{11}^-$

Substituting $N_x in the equation$,

$$U = \frac{1}{2} b \bar{A_{(11)}}^2 [\frac{I_1}{A_{11}} + \frac{I_2}{D_{11}}] \tag{3.38}$$

The strain energy of equivalent panel

$$U = \frac{1}{2} (2c) b A_{11}^- \tag{3.39}$$

$$U = bc A_{11}^- \tag{3.40}$$

Since strain energy for both corrugated panel and equivalent panel are the same,

$$A_{11}^- = \frac{2c}{\frac{I_1}{A_{11}} + \frac{I_2}{D_{11}}}$$

Similarly;

$A_{22}^-, A_{66}^-, D_{11}^-, D_{22}^-, D_{66}^- are found.$

In order to calculate the equivalent model for round corrugation, the following formulae are used.

Half length

$$(l) = \pi R + 2L \tag{3.41}$$

$$I_1 = \pi R \tag{3.42}$$

$$I_2 = \frac{4L^3}{3} + 2\pi L 2R + 8LR^2 + \pi R^3 \tag{3.43}$$

$$C = 2R \tag{3.44}$$

Equivalent plate stiffness matrices elements are calculated as below

$$A_{\bar{1}\bar{1}} = \frac{2c}{\frac{I_1}{A_{11}} + \frac{I_2}{D_{11}}} \tag{3.45}$$

$$A_{\bar{1}\bar{2}} = \frac{A_{12}}{A_{11}} A_{11} \tag{3.46}$$

$$A_{\bar{2}\bar{2}} = A_{12}\frac{A_{12}}{A_{11}} + \frac{(A_{11}A_{22} - A_{12}^2)}{A_{12}}\frac{l}{2R} \tag{3.47}$$

$$A_{\bar{6}\bar{6}} = \frac{2R}{l} A_{66}$$

$$D_{\bar{1}\bar{1}} = \frac{2R}{l} D_{11} \tag{3.48}$$

$$D_{\bar{1}\bar{2}} = \frac{D_{12}}{D_{11}} D_{11} \tag{3.49}$$

$$D_{\bar{2}\bar{2}} = \frac{l}{2C}[I_2 A_{22} + I_1 D_{22}] \tag{3.50}$$

$$D_{\bar{6}\bar{6}} = \frac{l}{2R} D_{66} \tag{3.51}$$

Using the equivalent stiffness matrices elements , the equivalent young's modulus in fiber direction can be calculated as follows

We know,

$$\mathrm{A}_{\bar{1}\bar{1}} = \frac{2c}{\frac{I_1}{A_{11}} + \frac{I_2}{D_{11}}}$$

substituting equation 3.41,3.42, 3.43 along with the following equations

$$A_{11} = Q_{\bar{1}\bar{1}} t \tag{3.52}$$

$$D_{11} = \frac{1}{3} Q_{1\bar{1}} t^3 \tag{3.53}$$

We get,

$$A_{\bar{1}\bar{1}} = \frac{2CQ_1{}_1^{t^3}}{t^2 I_1 + 3I_2} \tag{3.54}$$

Then,

$$Q_{\bar{1}\bar{1}} = \frac{A_1{}_1^{t^2 I_1 + 3I_2}}{2Ct^3} \tag{3.55}$$

Also,

$$Q_{\bar{1}\bar{1}} = \frac{E_1}{(1 - \nu_{12}\nu_{21})} \tag{3.56}$$

So,

$$E_1 = \frac{Q_1{}_1^{(1-\nu_{12}\nu_{21})}}{\nu_{12}} \tag{3.57}$$

Similarly, To calculate equivalent young's modulus in transverse direction, the following steps are followed as

$$A_{\bar{1}\bar{2}} = \frac{A_{12}}{A_{11}} A_{11} \tag{3.58}$$

substituting

$$A_{12} = Q_{12} t \tag{3.59}$$

$$A_{11} = Q_{11} t \tag{3.60}$$

$$D_{11} = \frac{1}{3} Q_{\bar{1}\bar{1}} t^3 \tag{3.61}$$

as well as 3.44, 3.41, 3.42, 3.43 We get,

$$A_{\bar{1}\bar{2}} = \frac{2CQ_{\bar{1}\bar{2}} t^3}{(t^2 I_1 + 3I_2)} \tag{3.62}$$

$$Q_{\bar{1}\bar{2}} = \frac{A_{\bar{1}\bar{2}} (t^2 I_1 + 3I_2)}{2Ct^3} \tag{3.63}$$

Also,

$$Q_{\bar{1}\bar{2}} = \frac{\nu_{12} E_2}{(1 - \nu_{12}\nu_{21})} \tag{3.64}$$

$$E_2 = \frac{Q_{\bar{1}\bar{2}} * (1 - \nu_{12}\nu_{21})}{\nu_{12}} \tag{3.65}$$

Shear modulus for both directions are

$$G_{12} = \frac{E_1}{2(1 + \nu_{12})} \tag{3.66}$$

$$G_{21} = \frac{E_2}{2(1 + \nu_{21})} \tag{3.67}$$

3.4 Edgewise Crush Test

The edgewise crush test is a compression test that is routinely carried out to check the corrugated board quality. This test comprises of holding the corrugated board vertically between two clamps and applying force in the plane on the edges or along the axis.

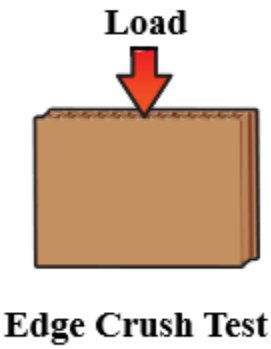

Figure 3.8. Edge Crush test [19]

Deformation progresses till the corrugated board fails after a sufficient amount of strain due to out of plane crease or local buckling. Based on this test, the ECT value of the board is calculated which determines the pounds per linear inch of load bearing edge. [5], [20]

As cardboard is an orthotropic material, the strength in in-plane direction parallel to the loading (machine direction) & in-plane direction normal to machine direction (cross direction) have different values of ECT. Performing the edgewise crush test in both directions provides the quality of the board without performing the box compression test.

In this paper, edgewise crush test is performed on the equivalent model of both profiles (B & C) for both directions (machine direction & cross direction). A comparative study is carried out between the Flax FRP skins with corrugated cardboard core specimen and the corrugated cardboard boxes to determine the increase or decrease in ECT value.

In this paper, edgewise crush test is performed on the equivalent model of both profiles (B & C) for both directions (machine direction & cross direction). A comparative study is carried out between the Flax FRP skins with corrugated cardboard core specimen and the corrugated cardboard boxes to determine the increase or decrease in ECT value. There are four methods based on the boundary conditions and shape of the specimen. The four methods are a) Edge- clamping method

b) Neck down method

c) Rectangular test specimen method with small slenderness ratio

d) Edge reinforced method (wax coating) [5]

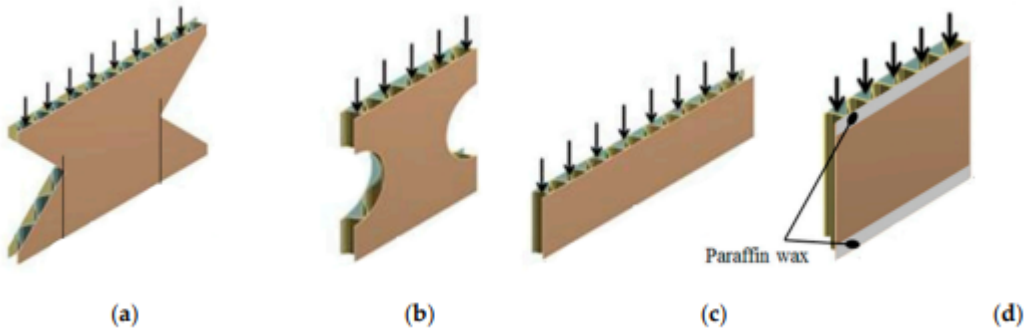

Figure 3.9. Methods of Edge Crush Test [21]

In this paper, the edge crush test is performed through the edge clamping method. In this method, clamps are used to hold the specimen in place and load is applied on the top edge with a loading rate of 12.5 ± 0.25 mm/min. A comparative study is carried out between both specimens for both directions to determine the best specimen with the help of load vs deformation plot.

3.5 Flat Crush Test / Mullen Burst Test

Similar to the edgewise crush test, another test is also performed to check the compression quality of the corrugated cardboard. This test is called the flat crush test or the Mullen burst test. The edgewise crush test is carried out to calculate the in plane compressive stresses whereas the flat crush test is carried out to calculate the out of plane compressive stresses.

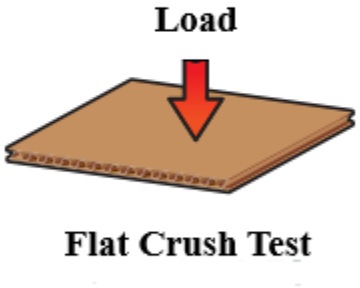

Figure 3.10. Methods of Edge Crush Test [19]

The flat crust test has the same loading rate as that of the edgewise crush test which is 12.5 ± 0.25 mm/min. Similar to the edgewise crush test, the flat crush test is also performed on both flutes (B & C) for both specimens. A comparative study is carried out to conclude whether the flax fiber reinforced skins with corrugated core is an alternative option to all cardboard specimens.

3.6 Four Point Bending Test

The four point bending test provides flexural deflection response of the material on application of load applied from out of plane. The test is setup with a loading span proportional to the supporting span. The loading span was selected to be equal to (2/11) of the supporting span.

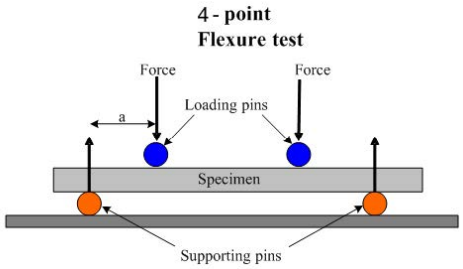

Figure 3.11. Methods of Edge Crush Test [22]

The test is performed using a fixed rate of 2 mm/min and values along the applied load are measured every 1 second for data processing. In this paper, both specimens undergo four point bending to compare the flexural stiffness.

Along with this, a thicker cardboard core specimen is modelled with flax fiber reinforced polymer skin to replicate the specimen used in the reference paper. The loading rate is kept similar and the load vs deflection graph is plotted to validate the material properties and the finite element analysis performed in this paper to derive a conclusion.

4. FINITE ELEMENT ANALYSIS

4.1 Material Properties

Two unique cardboard flutes are used in the fabrication of the sandwich cardboard boxes viz. B & C. each flute type has a nominal thickness which is basically the height of the flute and the density for each flute also differs.

Unidirectional flax fabric is used with an aerial weight of 275 g/m2. These fibers are used to fabricate fiber reinforced polymer skins with the help of a bio based resin called as Super Sap One. This resin has 30% bio content and is reported to have a tensile strength, modulus elongation of 53.23 MPa, 2.65GPa and 6% respectively. The flax fiber reinforced polymer skin samples made with the bio based epoxy have an average tensile strength initial modulus of 198 ± 9.3 MPa and 17.09 ± 0.63 GPa. The skin has two layers both being at an angle of 0. The thickness of both layers together is 1.97 ± 0.009mm. The secondary modulus is 11.93 ± 0.39 GPa. The rupture strain is reported to be 0.0153 ± 0.0006mm/mm [23].

The Cardboard specimen used cardboard as the skin with corrugated cardboard as the core. The material properties for the cardboard are as below.

Table 4.1. Cardboard Material Properties [24]

Material Properties	Value
E_1	7.6 GPa
E_2	4.02 GPa
E_3	0.038 GPa
ν_{12}	0.34
ν_{21}	0.01
ν_{13}	0.01
G_{12}	2.14 GPa
G_{21}	0.02 GPa
G_{13}	0.07 GPa
ρ	404.5 kg/m^3

4.2 Specimen Preparation

According to Aidan McCracken and Pedram Sadegham[23], the first step in fabrication takes place by constructing cardboard cores. For the four point bending test , the cores are attached using a vegetable starch based adhesive called Tex-Tribond P- 1031. This adhesive is also used during the manufacturing of corrugated cardboard. The second step in the fabrication of the flax fiber reinforced polymer skins. The flax fabric is pre-cut and placed on a set of parchment paper that contains a layer of the bio based epoxy Super Sap One. The top layers of the flax fabric is then covered with epoxy to complete the skin. The corrugated cardboard core is then placed on the epoxy. This part of the specimen is first cured by placing a board on the core. After the bottom flax fiber reinforced polymer skin is cured, the skin is then applied to the other side and then cured as well. One specific rule is to be taken into consideration when curing the specimen. The flax fiber reinforced polymer skin is always placed at the bottom side to avoid the epoxy from seeping into the cardboard core. [23]

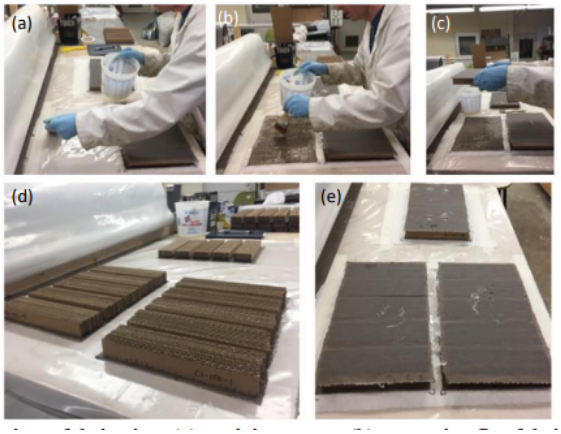

Figure 4.1. Fabrication of Flax fibre reinforced polymer skins
a)Applying epoxy to parchment paper
b)Placing flax fabric on the epoxy covering the other side with of the fabric with epoxy
c)Placing the corrugated cardboard core on the flax fabric
d)Curing completed on one side
e)Curing completed on both sides [23]

Material properties of the Flax fiber reinforced skin with corrugated cardboard core are mentioned below.

Table 4.2. Flax Fiber Reinforced Polymer Skin Material Properties [23]

Material Properties	Value
E_1	17.09 GPa
E_2	11.93 GPa
E_3	17.09 GPa
ν_{12}	0.46
ν_{21}	0.32
ν_{13}	0.46
G_{12}	15.82GPa
G_{21}	8.772 GPa
G_{13}	15.82 GPa
ρ	1540 kg/m^3

4.3 Geometry

The geometry of the corrugated cardboard core sandwich with flax fiber reinforced polymer skins as well as the corrugated cardboard core with cardboard skins is modelled using computer aided design software SOLIDWORKS. Following is the geometry of both specimens.

For B profile;

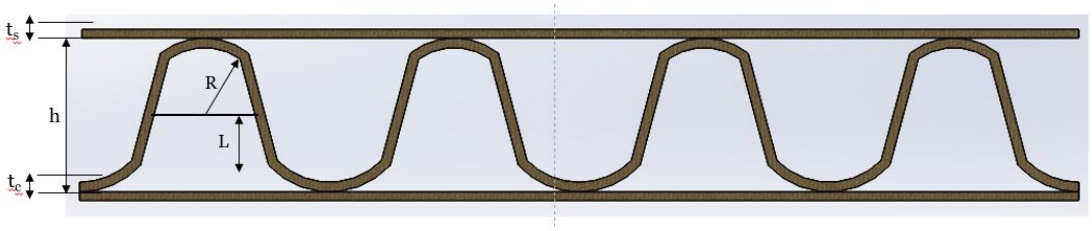

Figure 4.2. Dimensions of B profile corrugation

Table 4.3. Dimensions of B profile

Dimensions	Value(in mm)
Length of Corrugation (L)	1.52
Radius of Corrugation (R)	1.48
Height of corrugation	3.2
Thickness of corrugation	0.20
Thickness of skin	0.18
Width of skin	10
Length of skin	20.71

Equivalent model for B profile

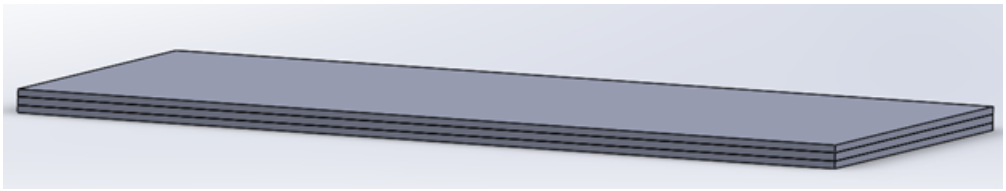

Figure 4.3. Equivalent model for B profile

Table 4.4. Dimensions of Equivalent model of B profile

Dimensions	Value(in mm)
Length (L)	20.71
Width of equivalent core (W)	10
Thickness of equivalent core	0.20
Thickness of skin	0.18
Width of skin	10
Length of skin	20.71

For C profile

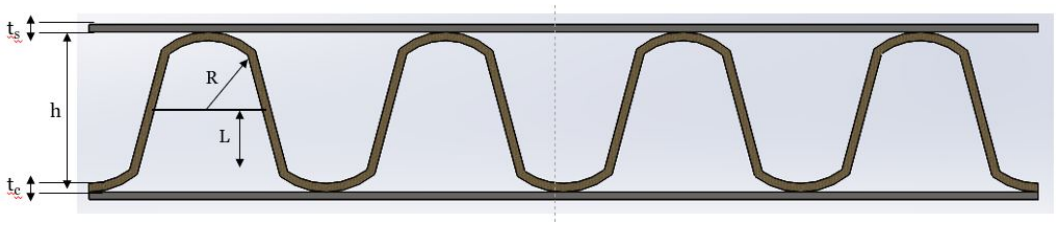

Figure 4.4. Dimensions of C profile corrugation

Table 4.5. Dimensions of C profile

Dimensions	Value(in mm)
Length of Corrugation (L)	2.29
Radius of Corrugation (R)	1.553
Height of corrugation	4.0
Thickness of corrugation	0.20
Thickness of skin	0.18
Width of skin	10
Length of skin	22.56

Equivalent model for C profile

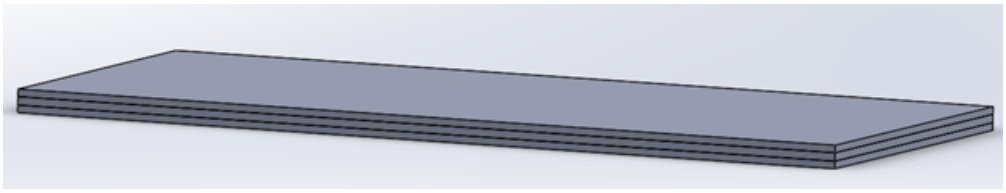

Figure 4.5. Equivalent model for C profile

Table 4.6. Dimensions of Equivalent model of C profile

Dimensions	Value(in mm)
Length (L)	22.56
Width of equivalent core (W)	10
Thickness of equivalent core	0.20
Thickness of skin	0.18
Width of skin	10
Length of skin	22.56

4.4 Finite Element Analysis

Finite element modelling and analysis for validating the equivalent models , edgewise crush test, mullen burst test and the four point bending test all are done using Finite Element Analysis software Ansys. All tests are done on both specimens for both flute profiles.

4.4.1 Homogenous Orthotropic Model with Equivalent Properties

In this test, the material properties of the equivalent model for the corrugated cardboard core is validated by performing a finite element analysis on both specimens (corrugated cardboard core with flax fiber reinforced polymer skins and equivalent model). Force of 10 N is applied normal to the skin for both specimens to measure the deformation.

Studies carried out on equivalent properties for orthortropic materials suggests that error occurred lies between a range of 5% to 20%. While peforming this finite element analysis, error in deformation is also calculated and the equivalent model with its properties are finalized for further analysis.

B profile

Geometry

Computer aided modelling is done in the well known computer aided sofware SOLIDWORKS. However, as the geometry for the corrugated cardboard core is complex, finite element modelling is carried out to simplify the model before meshing it.

Simplifying the model involves breaking down the model into smaller parts. These smaller parts are defined by separating the parts at complex curves in order to reduce the complexity of mesh at the curve where there is a possibility of it not meshing equidistantly.

Consideration is made to simplify the skins similar to the core as node merging is necessary for accurate results. Finite element modelling is carried out in Design Modeler. All the simplified parts are put together to form one entire part as the specimen is considered to act as one under application of force.

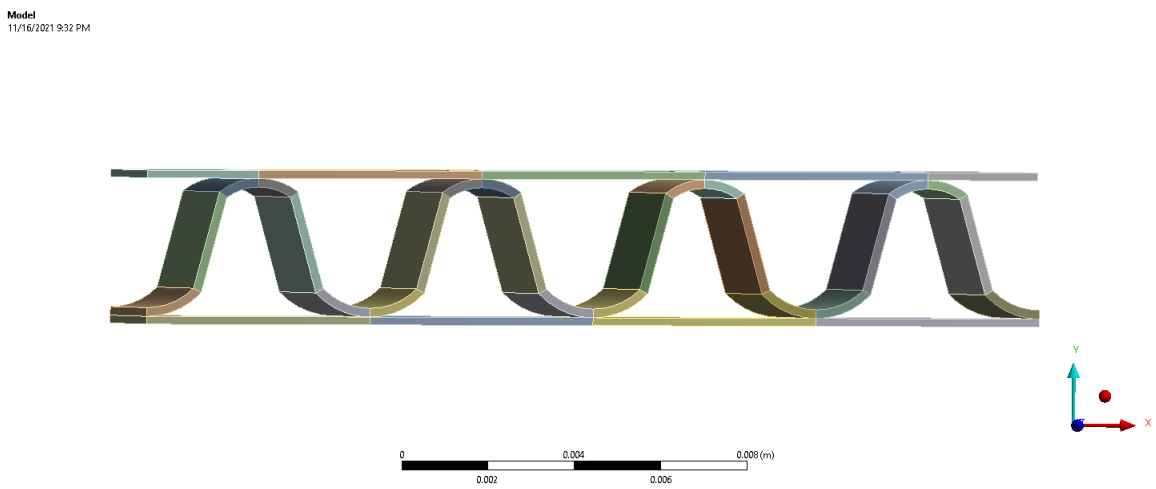

Figure 4.6. Finite element modelling of B profile

Mesh

Mesh is carried out in the finite element analysis software Ansys. The corrugated cardboard is the only complex geometry in the finite element model. As finite element modelling simplifies the part, meshing of these parts become easier.

Edge meshing is performed to divide each edge of the corrugated cardboard core as well as the skins in equal number of divisions. Multizone method meshing is done to create a mapped mesh which provides direction by using the curves as a source.

Table 4.7. Meshing statistics of B profile specimen

Nodes	Elements
8908	1170

Figure 4.7. Meshing statistics of B profile specimen

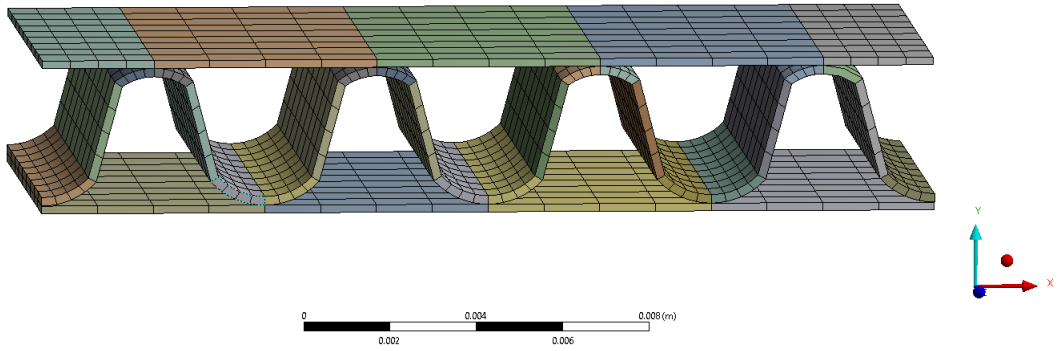

Figure 4.8. Multizone mesh of B profile

Boundary Conditions

The edges of the core and bottom flax fiber reinforced polymer skins are fixed in all three directions x.y.z and rotational directions, x,y,z. Force applied in Y direction is 10 N.

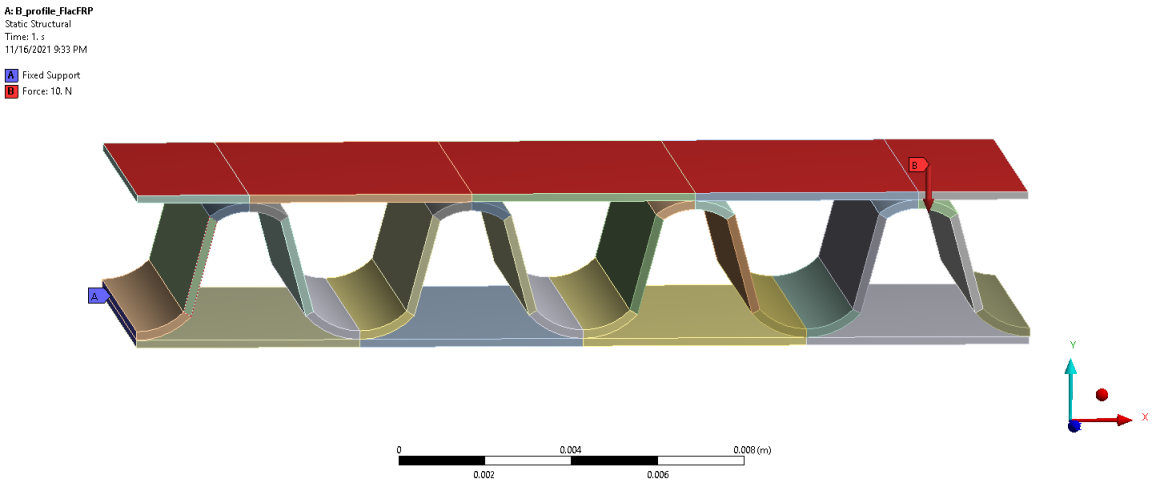

Figure 4.9. Boundary Conditions

Equivalent B profile

Geometry The Equivalent model for the corrugated cardboard core is a plate with similar dimensions in length, width and thickness. Equivalent properties calculated are used in this

finite element analysis. As the complex geometry is replaced, finite element modelling to simplify the model is not necessary. However, the skin and the core are considered as one part in this analysis.

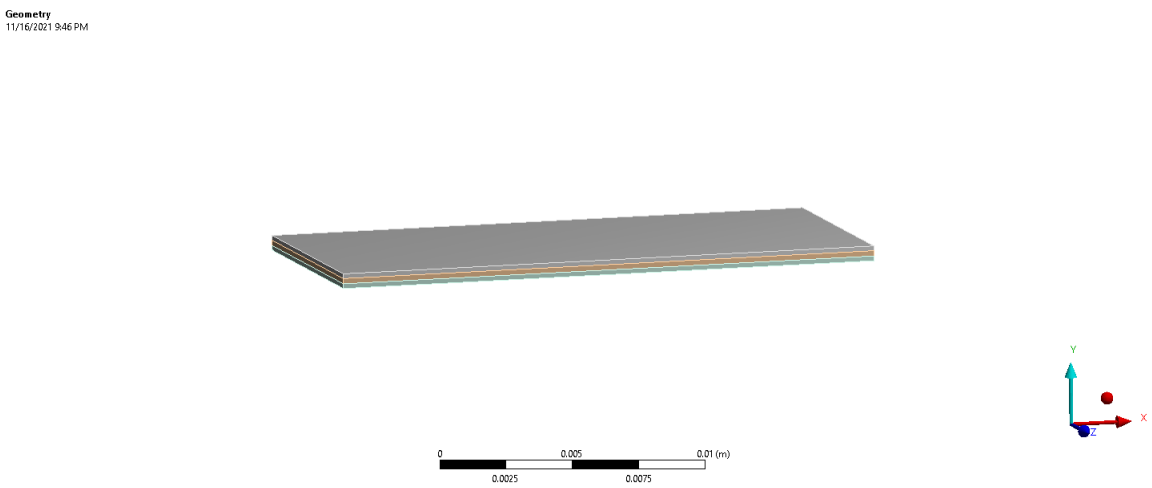

Figure 4.10. Equivalent model of B profile

Mesh

Mesh is carried out in the finite element analysis software Ansys. As the complex geometry is replaced by simple plate, mesh is done using body sizing for all three parts. Node merging is taken into consideration to provide accurate results.

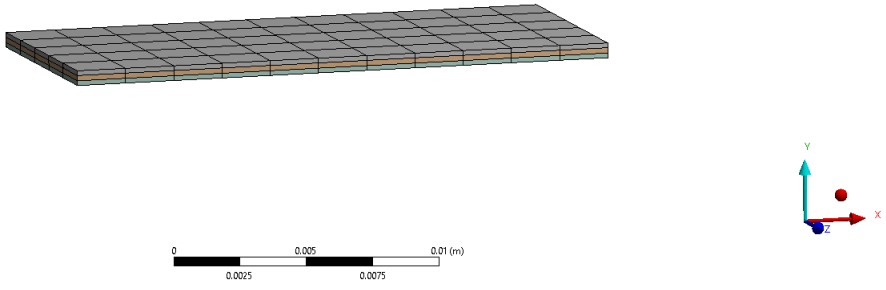

Figure 4.11. Mesh for Equivalent model of B profile

Table 4.8. Meshing statistics of B profile specimen

Nodes	Elements
1008	165

Boundary Conditions

The edges of the core and bottom flax fiber reinforced polymer skins are fixed in all three directions x.y.z and rotational directions, x,y,z. Force applied in Y direction is 10 N.

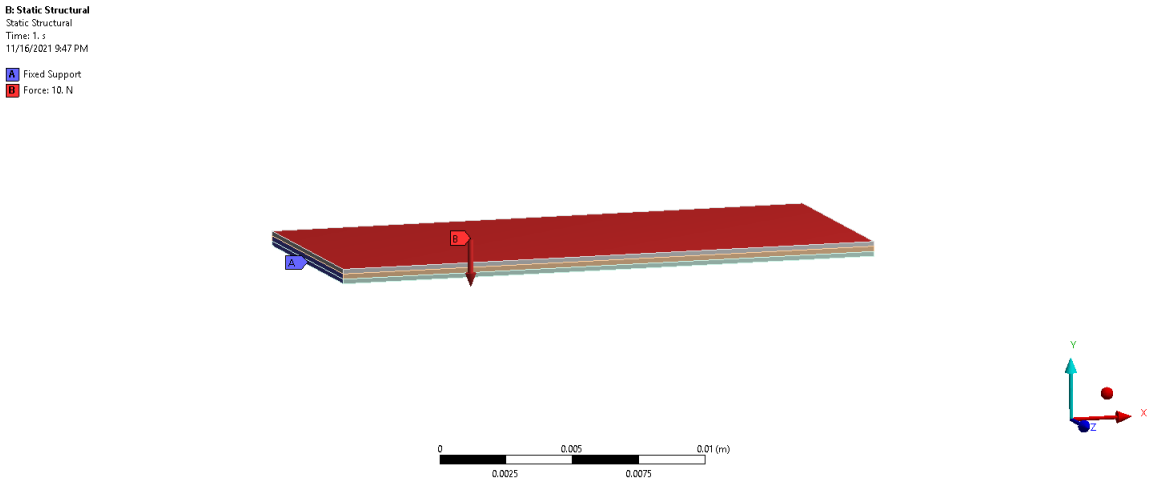

Figure 4.12. Boundary Conditions for equivalent model of B profile

C profile

Geometry

Computer aided modelling is done in the well known computer aided software SOLIDWORKS. However, as the geometry for the corrugated cardboard core is complex, finite element modelling is carried out to simplify the model before meshing it.
Simplifying the model involves breaking down the model into smaller parts. These smaller parts are defined by separating the parts at complex curves in order to reduce the complexity of mesh at the curve where there is a possibility of it not meshing equidistantly.

Consideration is made to simplify the skins similar to the core as node merging is necessary for accurate results. Finite element modelling is carried out in Design Modeler. All the simplified parts are put together to form one entire part as the specimen is considered to act as one under application of force.

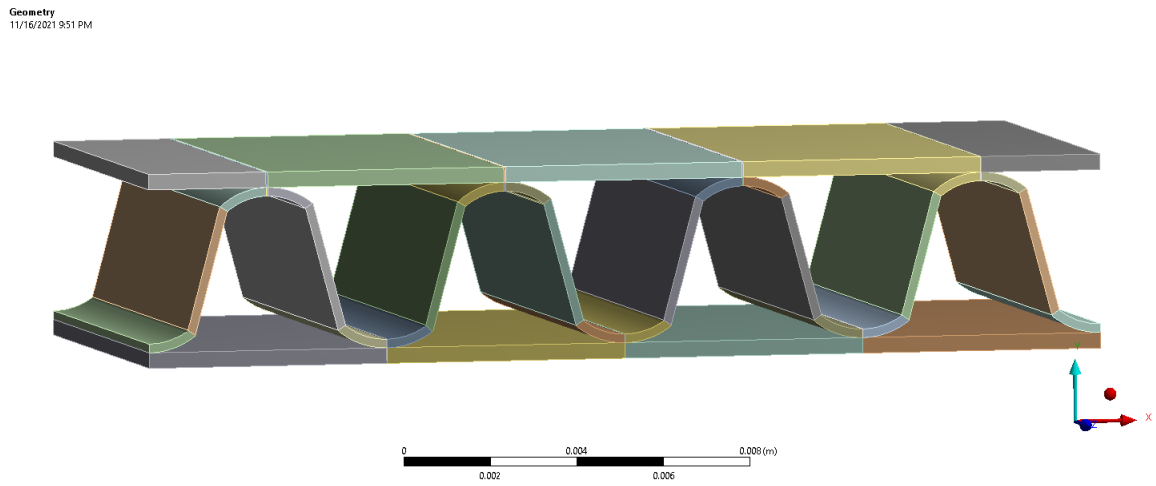

Figure 4.13. Finite element modelling of C profile

Mesh

Mesh is carried out in the finite element analysis software Ansys. The corrugated cardboard is the only complex geometry in the finite element model. As finite element modelling simplifies the part, meshing of these parts become easier.

Edge meshing is performed to divide each edge of the corrugated cardboard core as well as the skins in equal number of divisions. Multizone method meshing is done to create a mapped mesh which provides direction by using the curves as a source.

Figure 4.14. Meshing statistics of B profile specimen

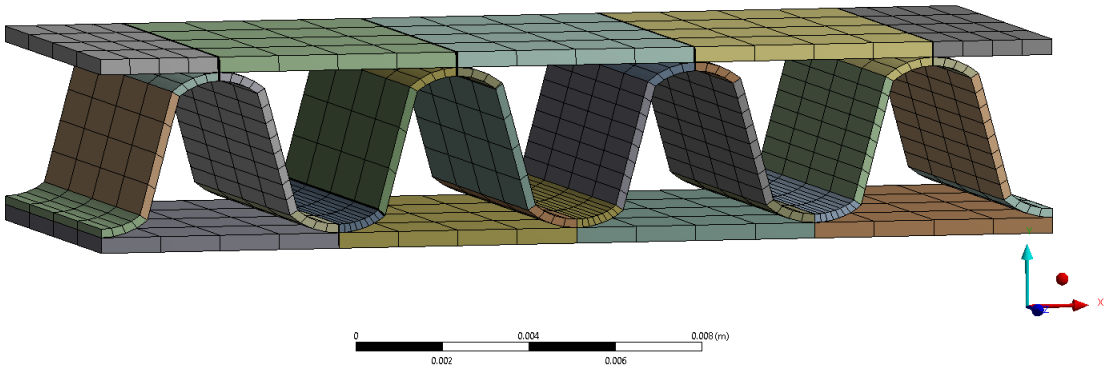

Figure 4.15. Mesh of C profile

Boundary Conditions

The edges of the core and bottom flax fiber reinforced polymer skins are fixed in all three directions x.y.z and rotational directions, x,y,z. Force applied in Y direction is 1000 N.

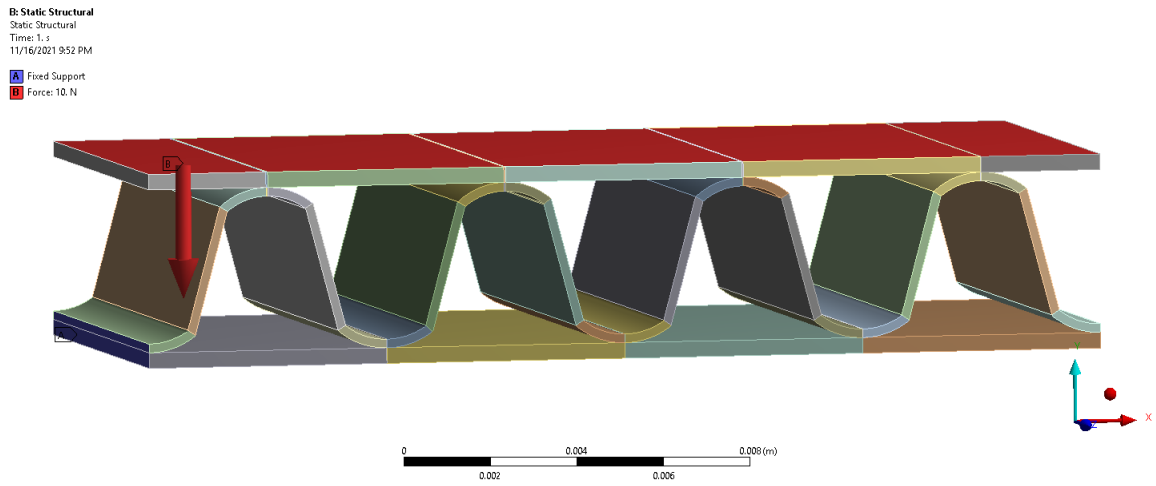

Figure 4.16. Boundary conditions of C profile

Equivalent model for C profile

Geometry

The Equivalent model for the corrugated cardboard core is a plate with similar dimensions in length, width and thickness. Equivalent properties calculated are used in this finite element analysis. As the complex geometry is replaced, finite element modelling to simplify the model is not necessary. However, the skin and the core are considered as one part in this analysis.

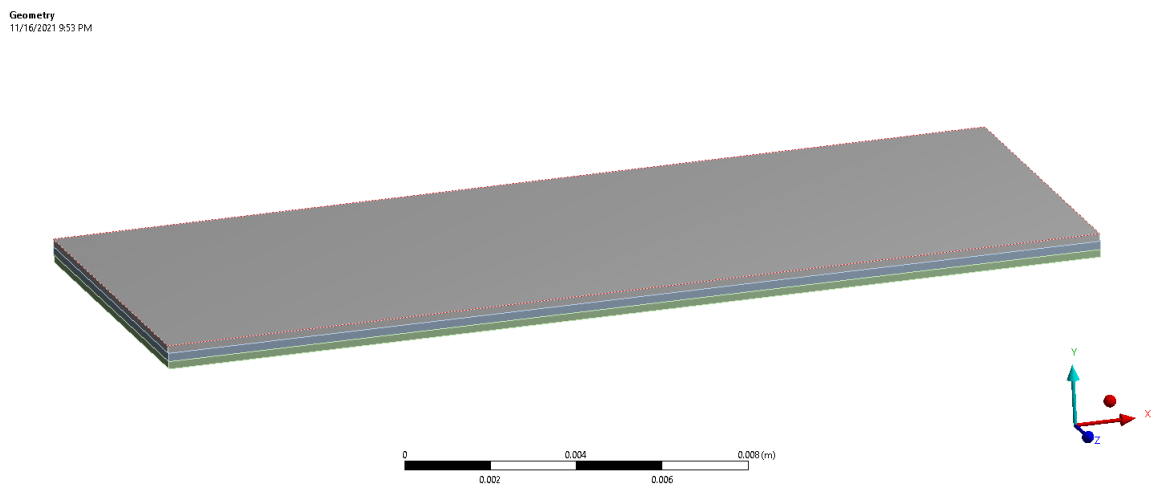

Figure 4.17. Equivalent model for C profile

Mesh

Mesh is carried out in the finite element analysis software Ansys. As the complex geometry is replaced by simple plate, mesh is done using body sizing for all three parts. Node merging is taken into consideration to provide accurate results

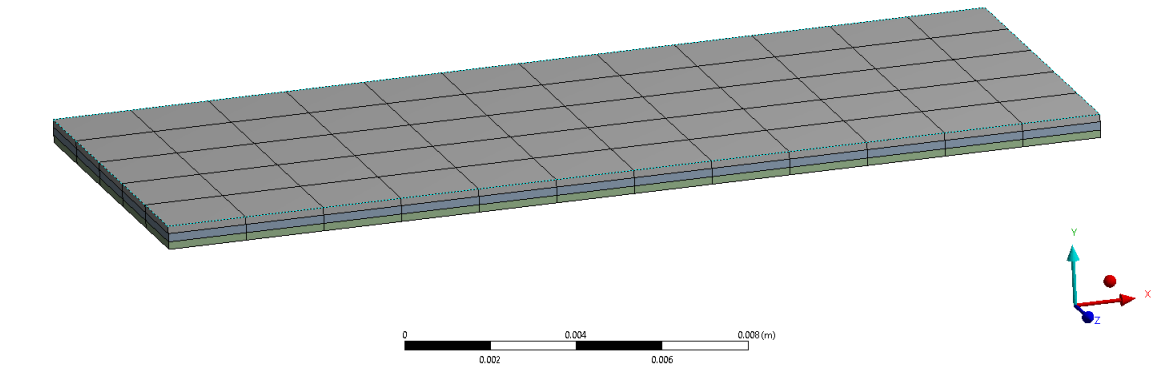

Figure 4.18. Mesh for Equivalent model for C profile

Boundary Conditions

The edges of the core and bottom flax fiber reinforced polymer skins are fixed in all three directions x.y.z and rotational directions, x,y,z. Force applied in Y direction is 1000 N.

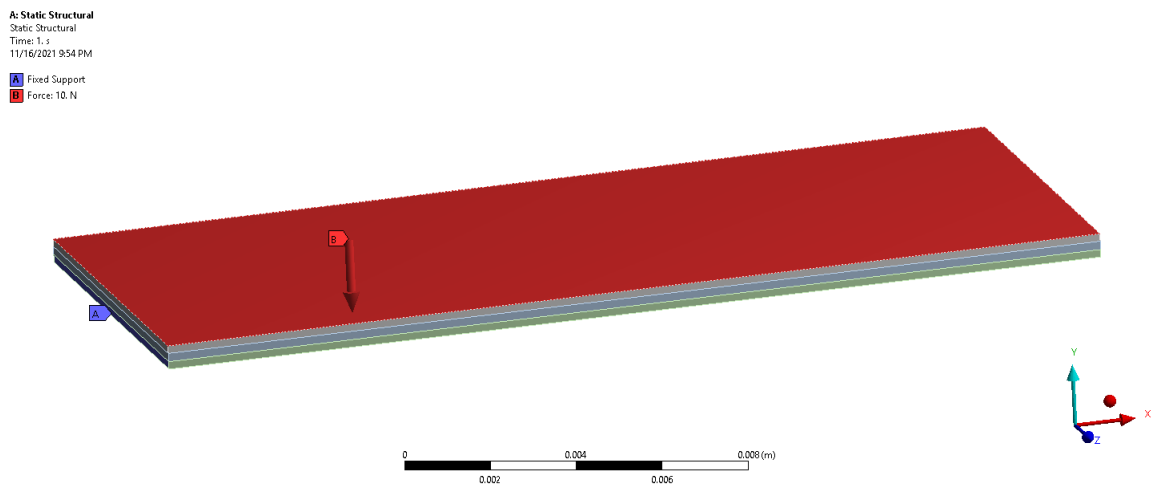

Figure 4.19. Boundary Conditions of Equivalent model for C profile

4.4.2 Edgewise Crush Test

Edgewise crush test is carried out in two different directions to represent the box compression test. In the edgewise crush test, the specimen is held between two clamps which are fixed. The top edge is loaded with force at a rate of 12.5 mm/min. Local buckling determines the failure in this test. Peak load is calculated to understand the amount of loading before failure. Load vs Deformation graph is plotted for both specimens for both profiles. The equivalent model is used for this analysis to reduce meshing elements and the computation time.

In Machine Direction

Boundary Conditions

The two clamps holding the specimen are fixed. The bottom edges of the specimen are also fixed to represent the experimental testing of the edge crush test. Force is applied on the top edge of the specimen.

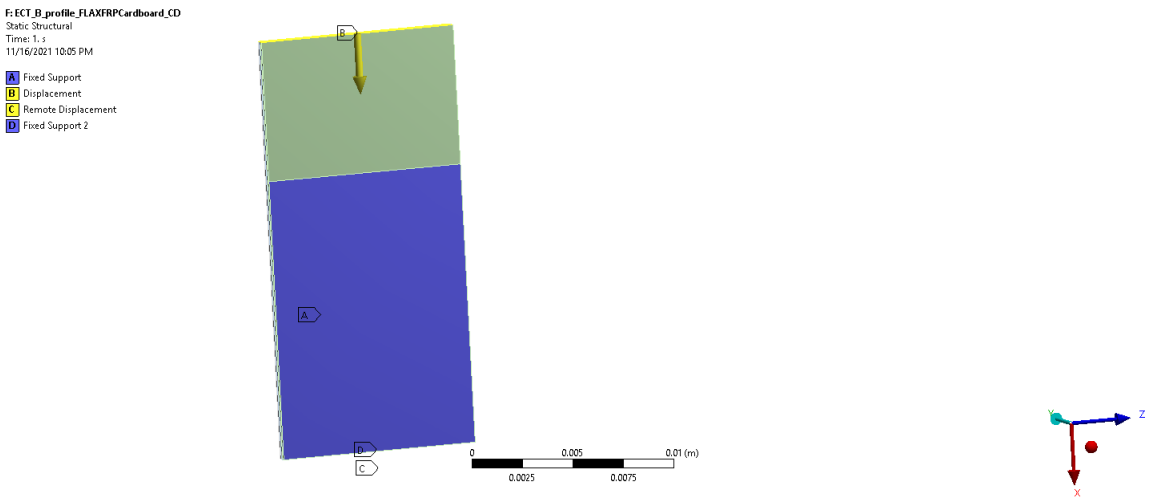

Figure 4.20. Boundary Conditions of Edge Crush test in Machine Direction

In Cross Direction

Boundary Conditions

The two clamps holding the specimen are fixed. The bottom edges of the specimen are also fixed to represent the experimental testing of the edge crush test. Force is applied on the top edge of the specimen.

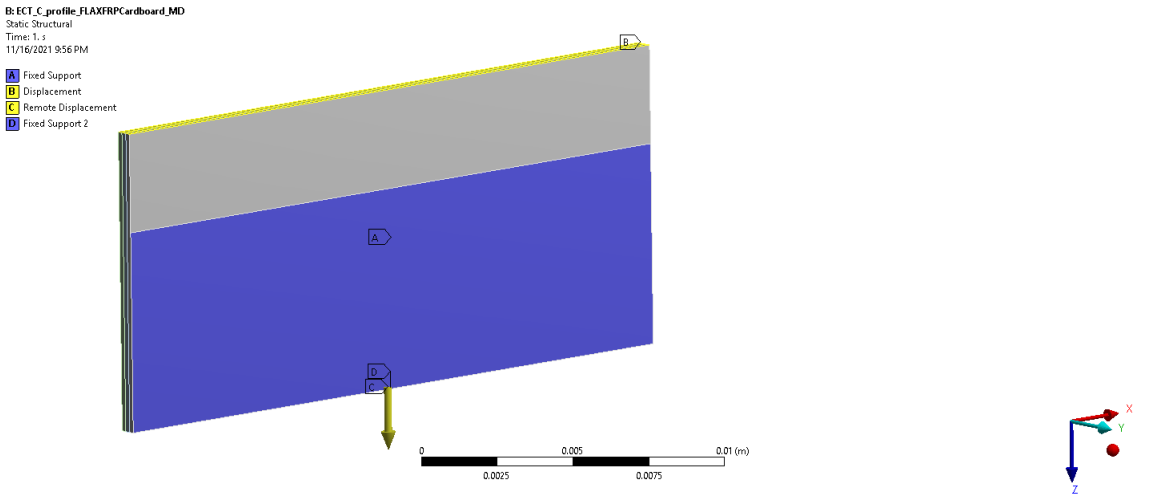

Figure 4.21. Boundary Conditions of Edge Crush test in Machine Direction

4.4.3 Flat Crush Test

Flat crush test is another test that checks the compression quality of the specimen. In the flat crush test, force is applied normal to the skin. This checks the compression quality of the corrugation. Complete compression of corrugation is considered as the failure in this test. While compression of corrugation takes place, indentation of the skin is also another failure that is taken into consideration.

Boundary Conditions

The specimen is placed between two sandpapers as the force is applied normal to the skin. If the bottom skin of the specimen is fixed , the compression on the bottom skin cannot be considered. Therefore, sandpaper is place to apply force equally on either sides. The bottom sandpaper is fixed. Force is applied on the top skin at a loading rate of 12.5 mm/min. Load vs deformation graoh is plotted to compare the results of both specimens for both profiles.

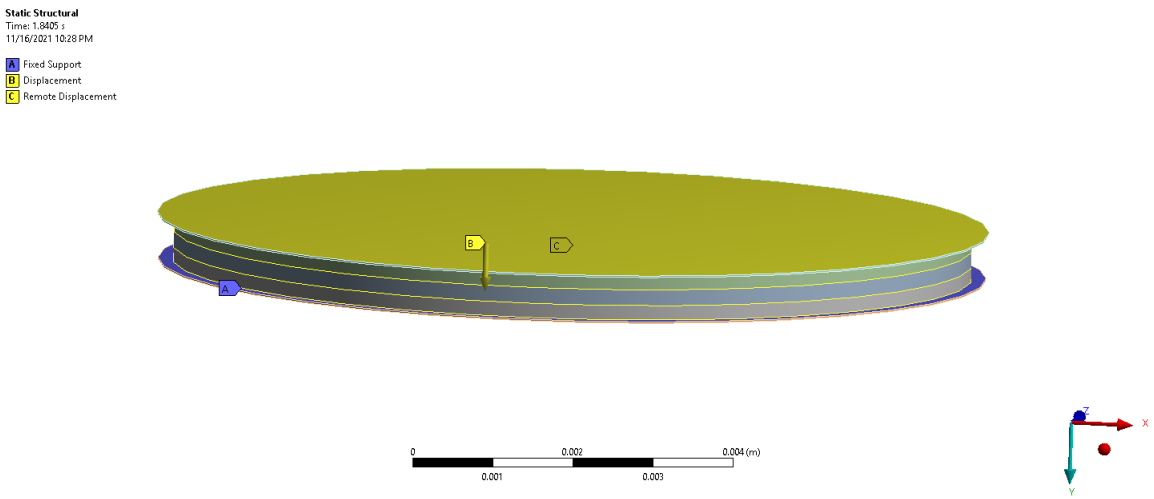

Figure 4.22. Boundary Conditions for Flat Crush Test

4.4.4 Four Point Bending Test

The four point bending test provides flexural deflection response of the material. The test is setup with a loading span proportional to the supporting span. The loading span was selected to be equal to (2/11) of the supporting span.

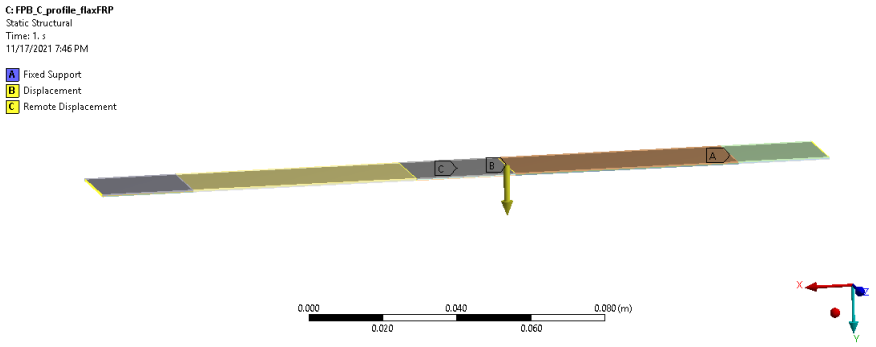

Figure 4.23. Boundary Conditions for Four point ending test

5. RESULTS

5.1 Homogenous Orthotropic Model with Equivalent Properties

B profile

The deformation of the specimen was calculated on application of force to validate the calculated equivalent material properties of the specimen.

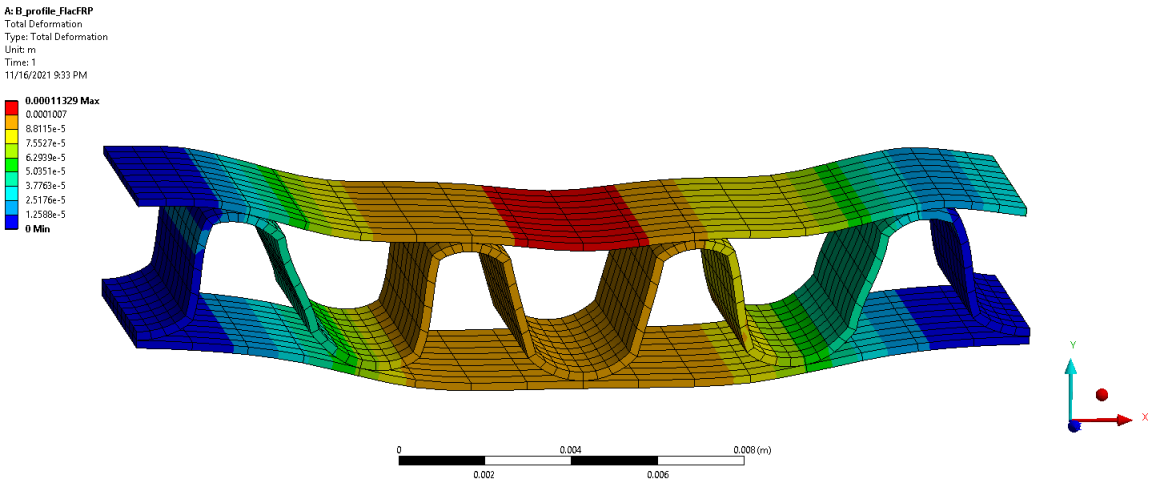

Figure 5.1. B profile deformation results

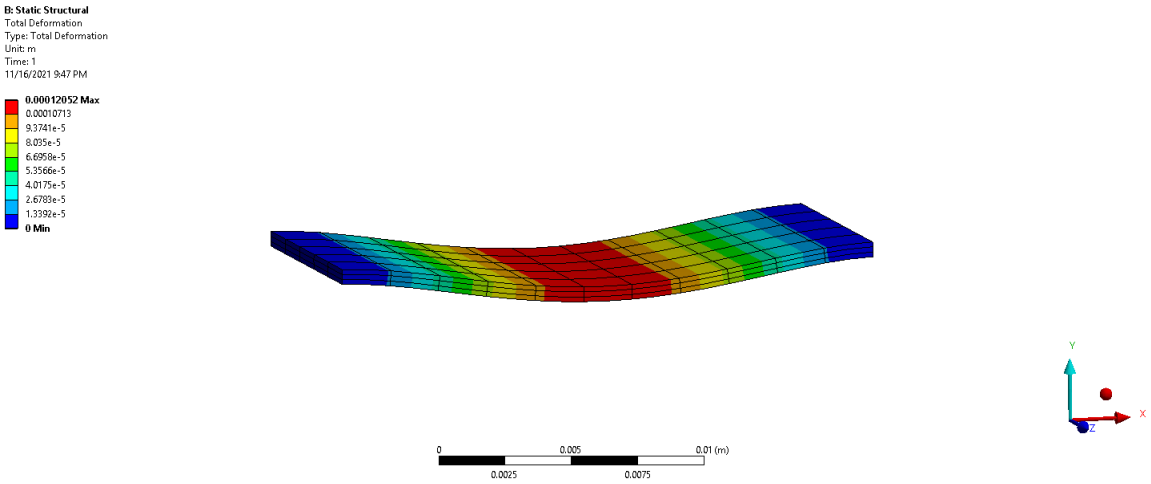

Figure 5.2. B profile equivalent model deformation results

Equivalent properties for B profile corrugated cardboard core is :

Table 5.1. Equivalent properties of B profile corrugated cardboard

Material Properties	Value
E_1	14.025 GPa
E_2	5.937 GPa
E_3	14.025 GPa
ν_{12}	0.34
ν_{21}	0.01
ν_{13}	0.01
G_{12}	15.2 GPa
G_{21}	2.998 GPa
G_{13}	15.2 GPa
ρ	404.5 kg/m^3

C profile

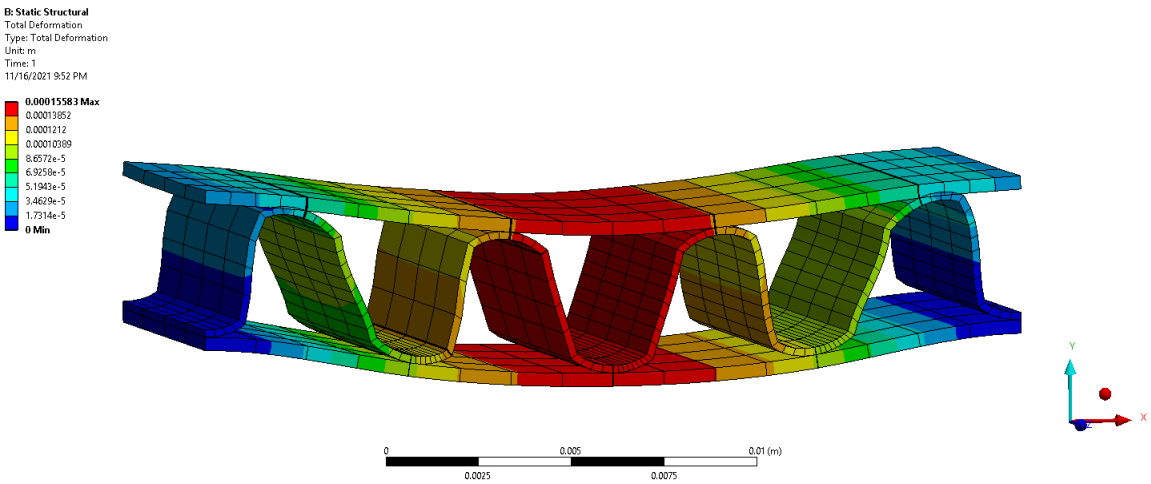

Figure 5.3. C profile deformation results

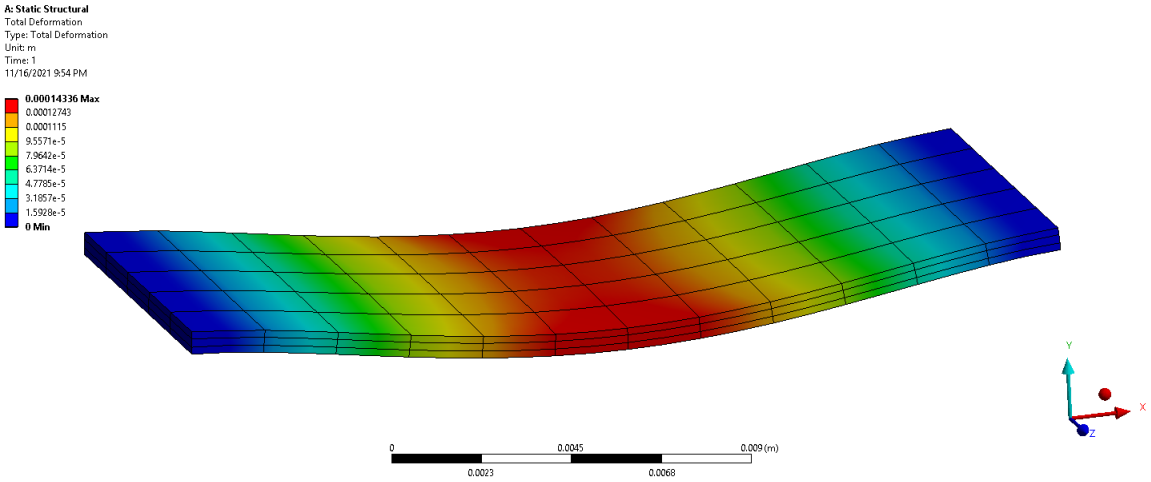

Figure 5.4. C profile equivalent model deformation results

Equivalent properties of C profile corrugated cardboard is :

Table 5.2. Equivalent properties of C profile corrugated cardboard

Material Properties	Value
E_1	25.02 GPa
E_2	8.91 GPa
E_3	25.302 GPa
ν_{12}	0.34
ν_{21}	0.01
ν_{13}	0.01
G_{12}	14.194 GPa
G_{21}	3.55391 GPa
G_{13}	14.194 GPa
ρ	404.5 kg/m^3

5.2 Edge Crush Test

B profile

In cross direction

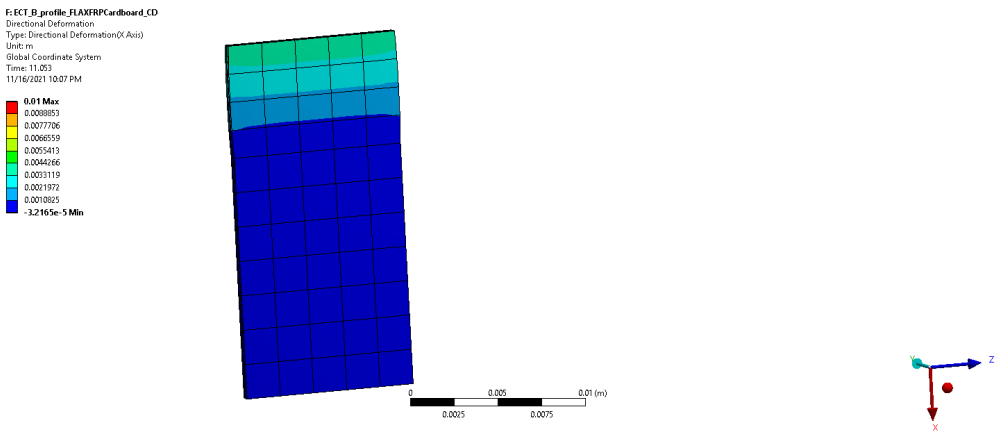

Figure 5.5. ECT for flax specimen in cross direction for B profile

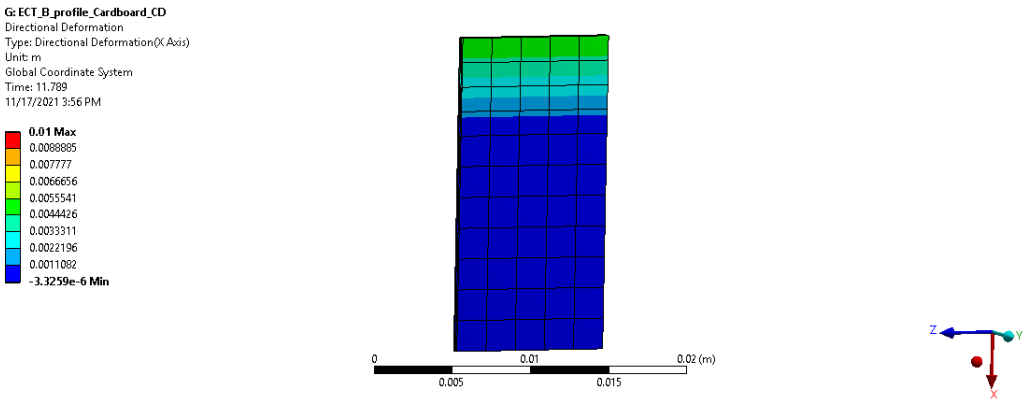

Figure 5.6. ECT for cardboard specimen in cross direction for B profile

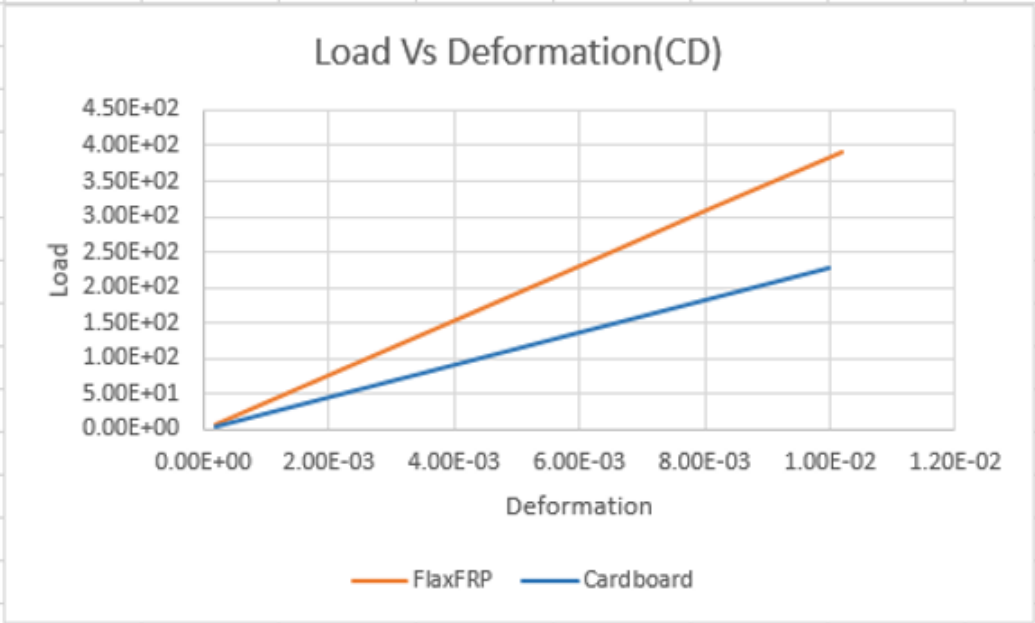

Figure 5.7. Load Vs Deformation in cross direction for B profile

In machine direction

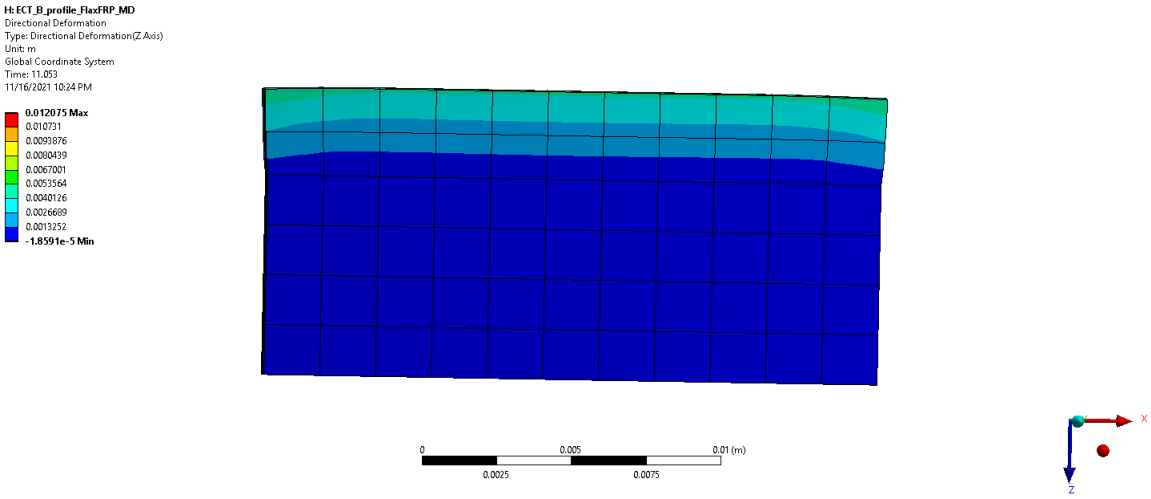

Figure 5.8. ECT for flax specimen in machine direction for B profile

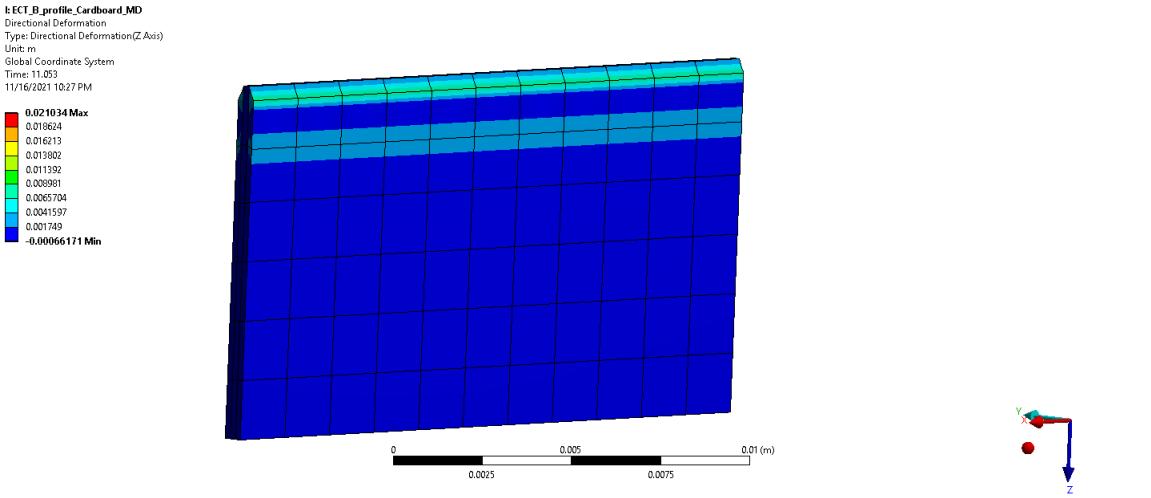

Figure 5.9. ECT for cardboard specimen in machine direction for B profile

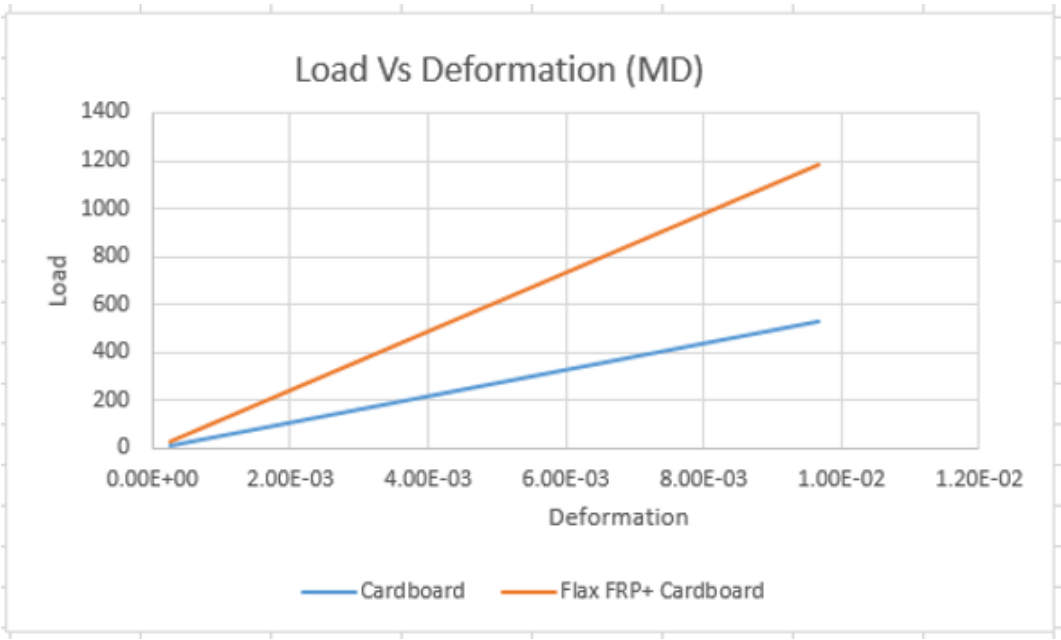

Figure 5.10. Load Vs Deformation in machine direction for B profile

C profile

In machine direction

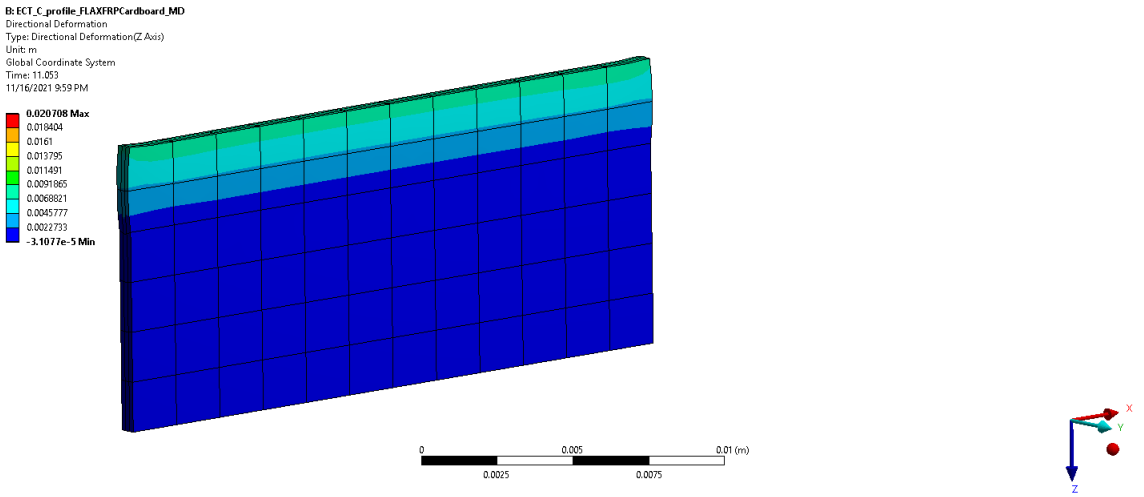

Figure 5.11. ECT for flax specimen in machine direction for C profile

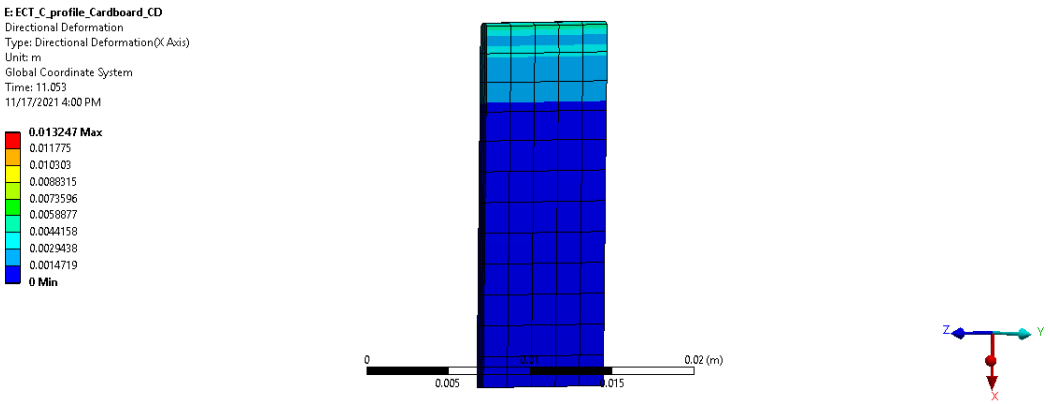

Figure 5.12. ECT for cardboard specimen in machine direction for C profile

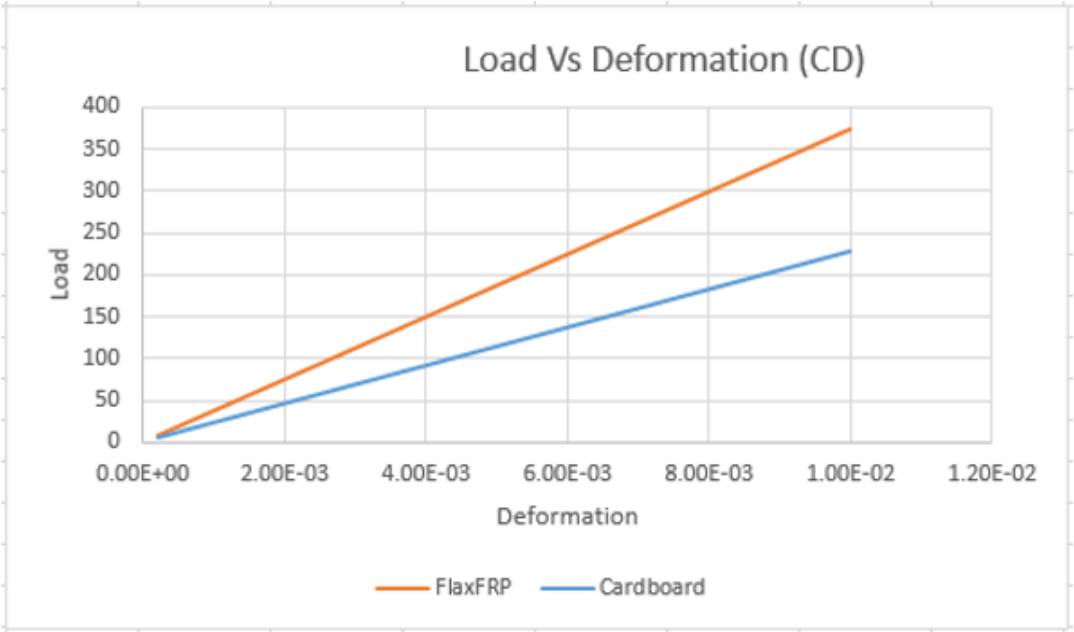

Figure 5.13. Load Vs Deformation in machine direction for C profile

In cross direction

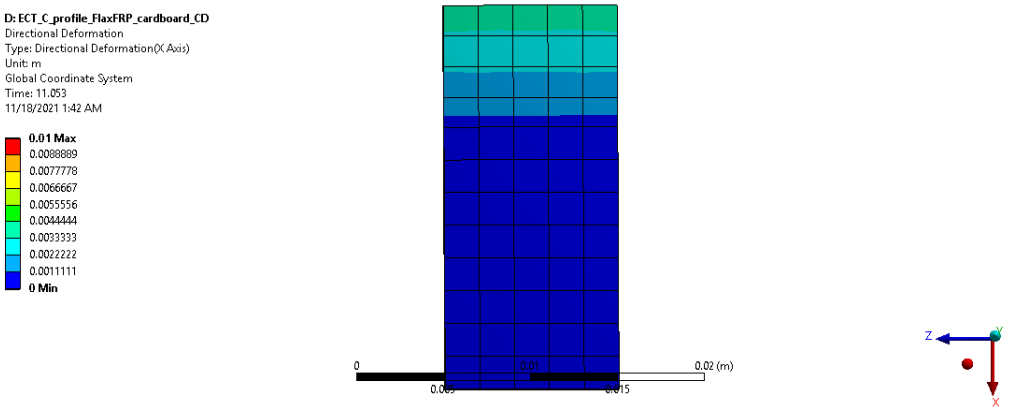

Figure 5.14. ECT for flax specimen in cross direction for B profile

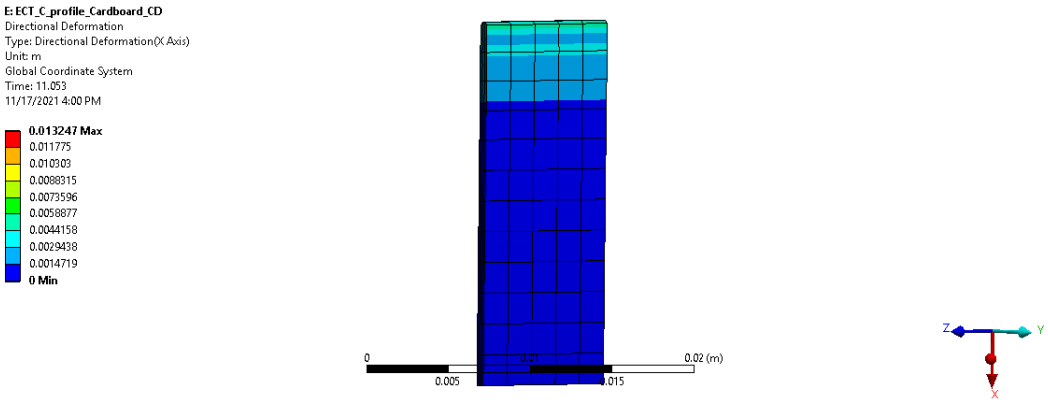

Figure 5.15. ECT for flax specimen in cross direction for B profile

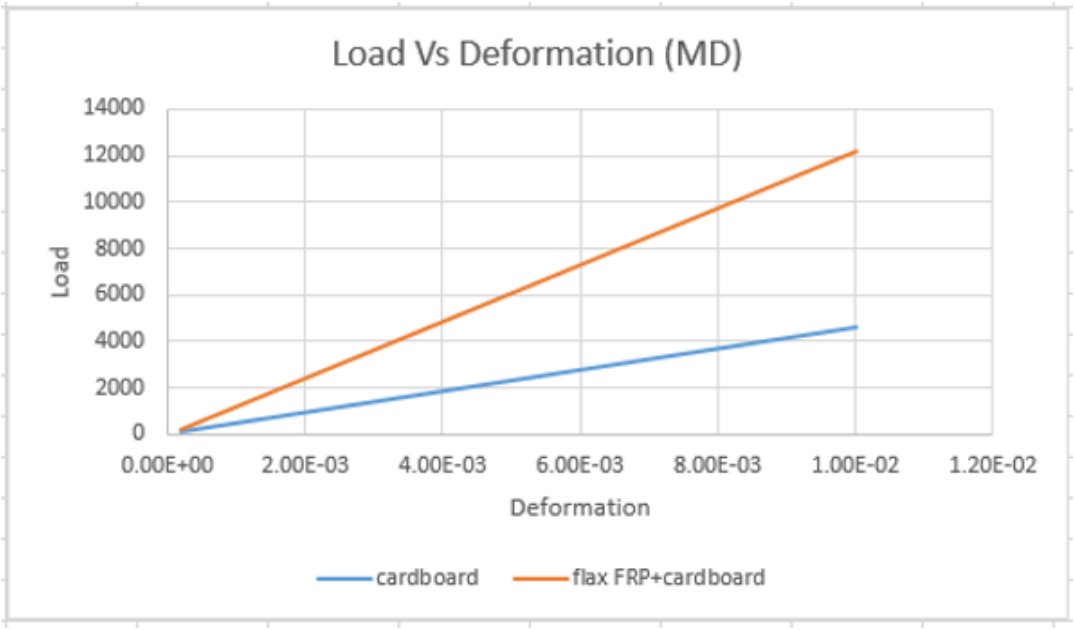

Figure 5.16. Load Vs Deformation in cross direction for C profile

5.2.1 Flat Crush Test

C profile

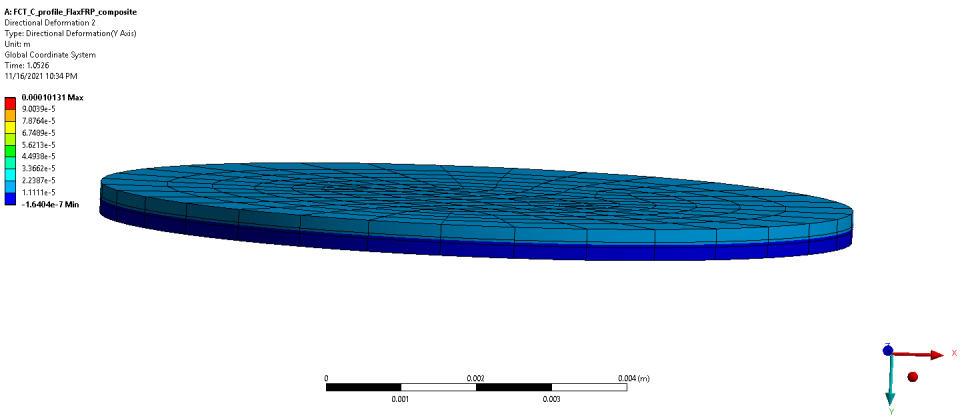

Figure 5.17. Flat crush test for C profile flax specimen

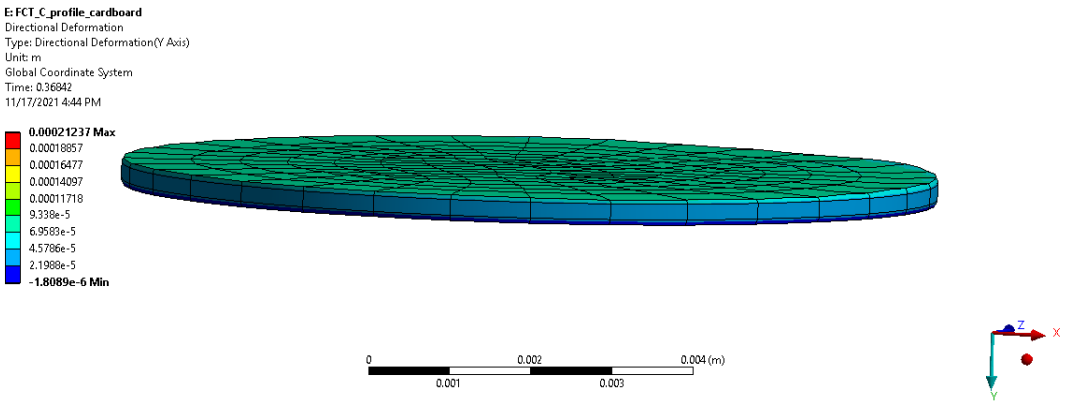

Figure 5.18. Flat crush test for C profile corrugated specimen

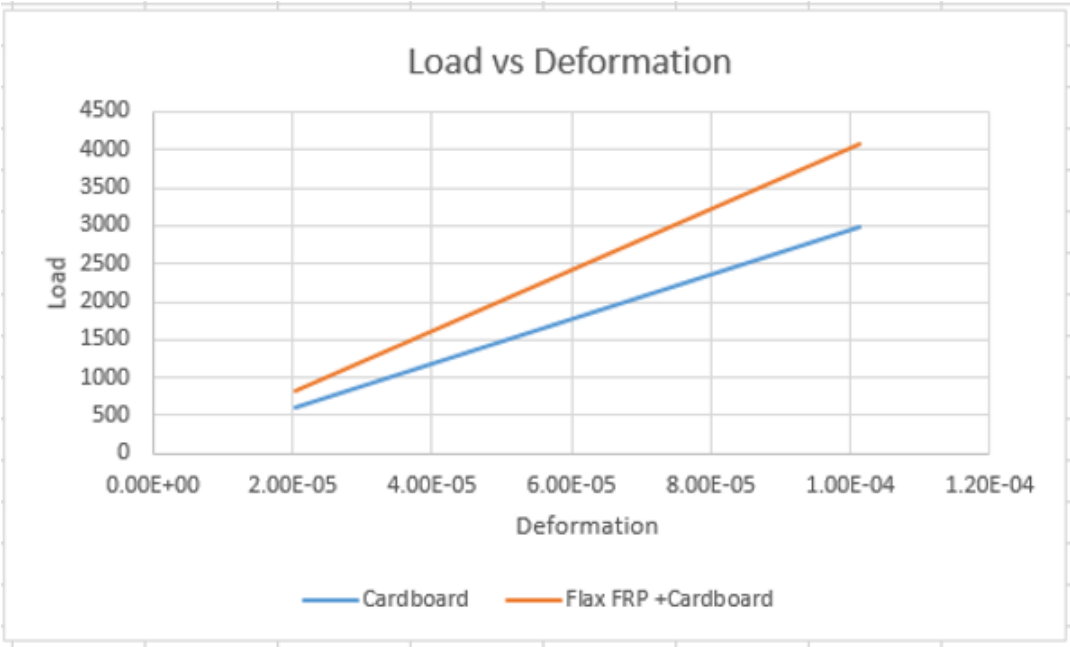

Figure 5.19. Load Vs Deformation for C profile

B profile

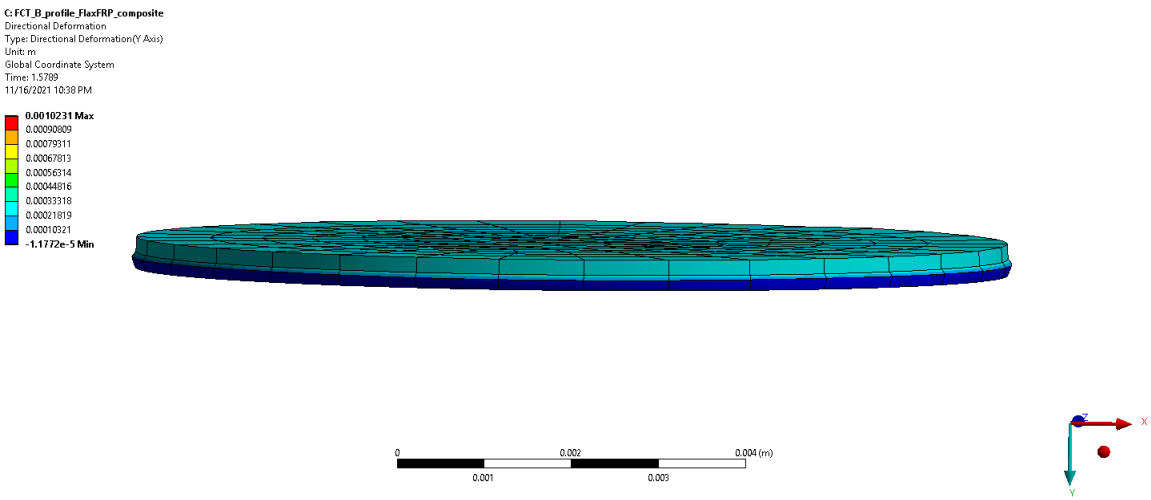

Figure 5.20. Flat crush test for B profile flax specimen

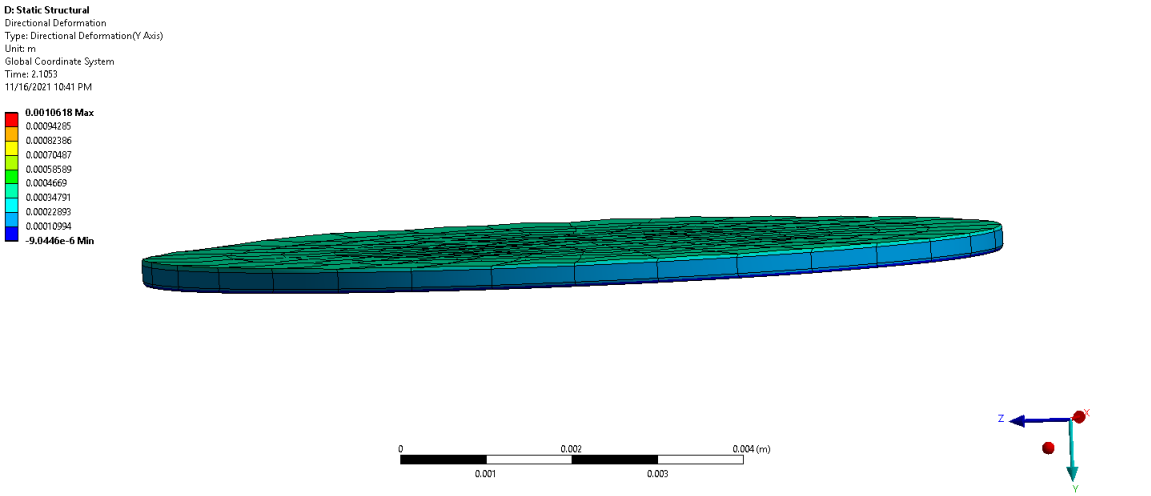

Figure 5.21. Flat crush test for B profile corrugated specimen

5.2.2 Four Point Bending Test

C profile

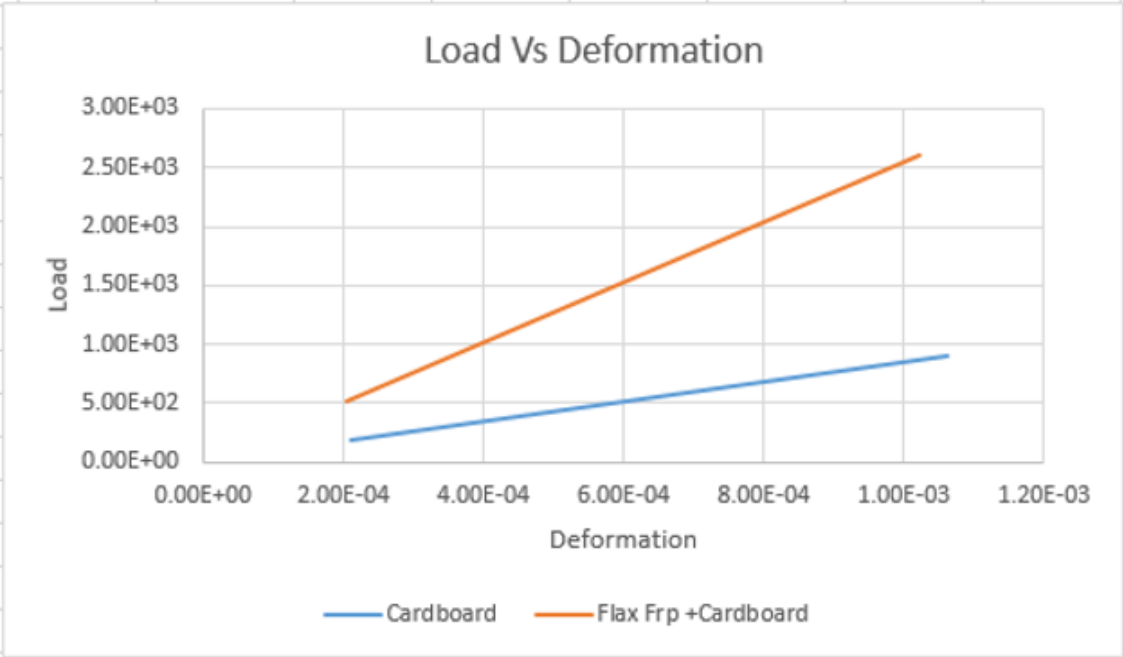

Figure 5.22. Load Vs Deformation for B profile

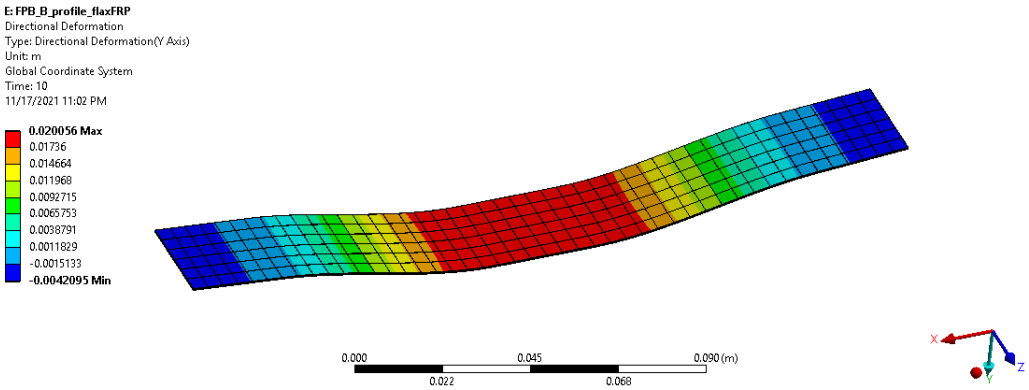

Figure 5.23. Four point bending deformation results for C profile for flax specimen

B profile

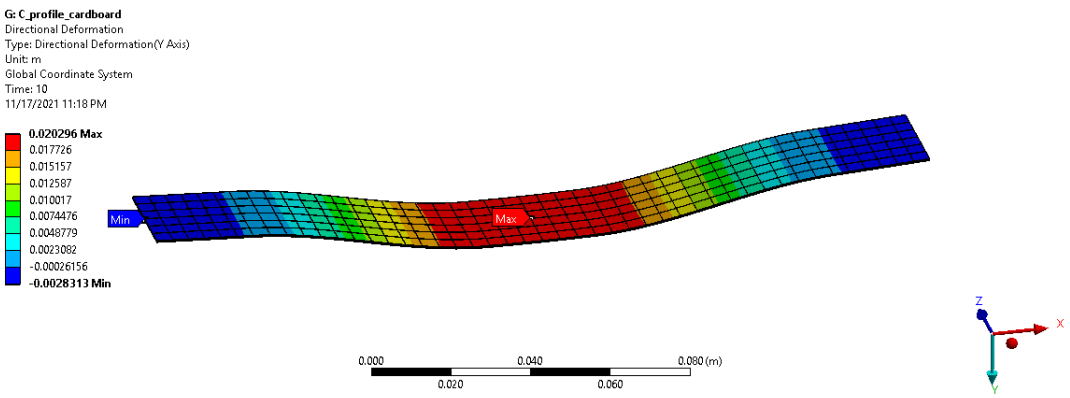

Figure 5.24. Four point bending deformation results for C profile for cardboard specimen

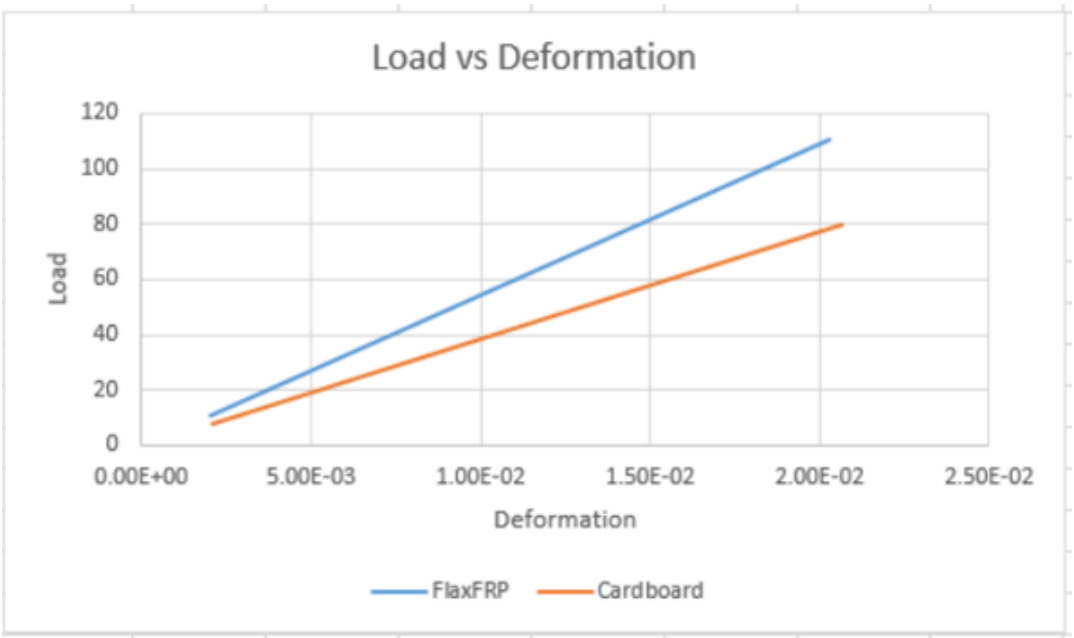

Figure 5.25. Load Vs Deformation for C profile

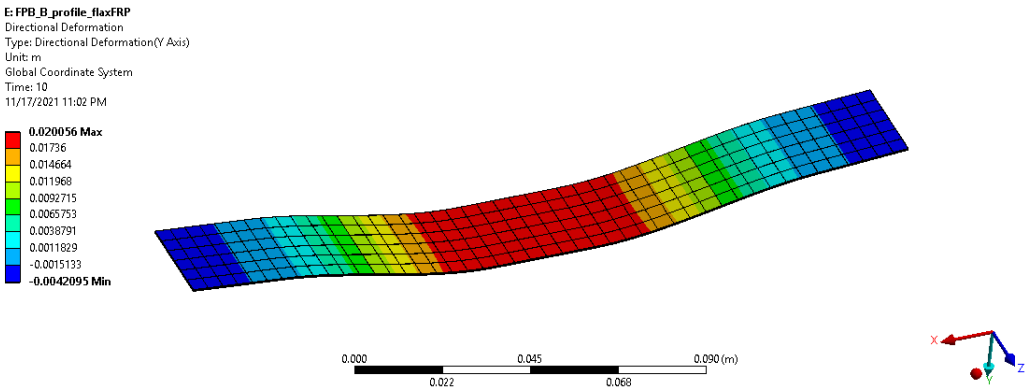

Figure 5.26. Four point bending deformation results for B profile for flax specimen

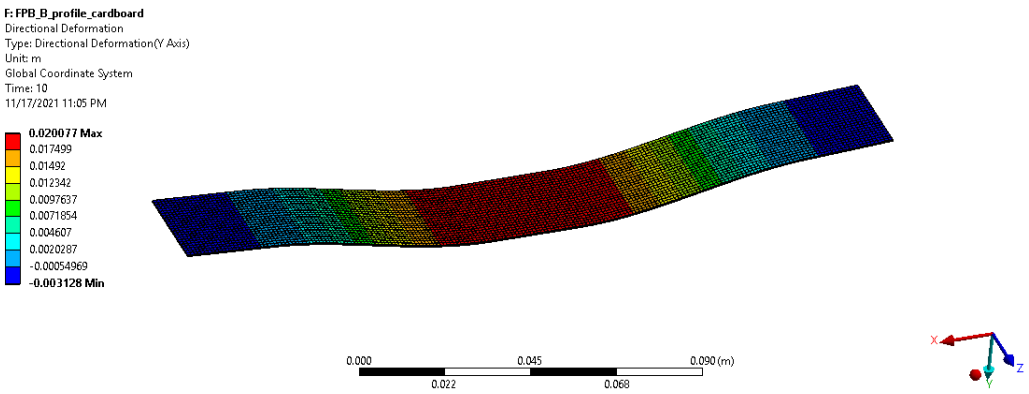

Figure 5.27. Four point bending deformation results for B profile for cardboard specimen

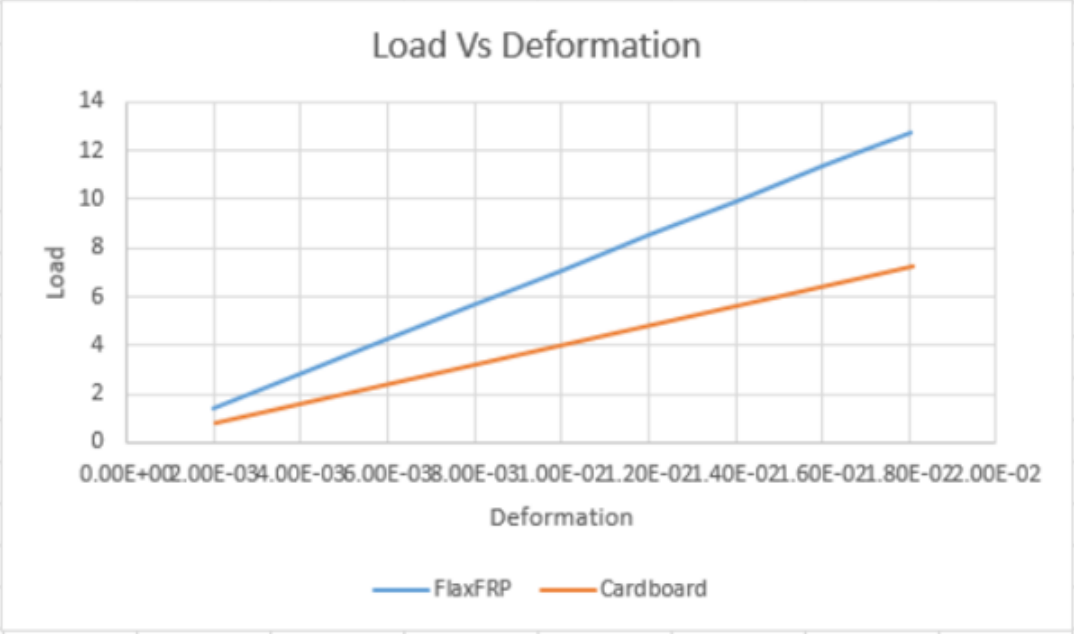

Figure 5.28. Load Vs Deformation for B profile

REFERENCES

[1] Andreas Allansson And Bjorn Svfrd, "Stability and collapse of corrugated board; numerical and experimental analysis," Master's Thesis, Lund University, 2001.

[2] W. Y. ZhengYe Victor L.Berdichevsky, "An equivalent classical plate model of corrugated structures," *International journal of Solid and Structures*, vol. 51, pp. 2073–2083, 2014. [Online]. Available: https://doi.org/10.1016/j.ijsolstr.2014.02.025.

[3] N. B. Marco Pierini Giorgio Bartolozzi, "Equivalent properties for corrugated cores of sandwich structures: A general analytical method," *Composite Structures*, vol. 108, pp. 736–746, Feb. 2014. [Online]. Available: https://doi.org/10.1016/j.compstruct.2013.10.012.

[4] D. Briassoulis, "Equivalent orthotropic properties of corrugated sheets," *Composite Structures*, vol. 2, pp. 129–138, 1986. DOI: https://doi.org/10.1016/0045-7949(86)90207-5.

[5] J. Park, M. Park, D. Choi, H. Jung, and S. Hwang, "Finite element-based simulation for edgewise compression behavior of corrugated paperboard for packaging of agricultural products," *Applied Sciences*, 2020. [Online]. Available: https://doi.org/10.3390/app10196716.

[6] *Flute profile for corrugated cardboard boxes*. [Online]. Available: earthenterprise.com/corrugated-boxes-facts.

[7] *Flute types*. [Online]. Available: https://www.productionpackaging.com.au/news/cardboard-flute-design-different-flutes-different-purposes.

[8] E. M. Reis, S. H., and Rizkallat, "Material characteristics of 3-d frp sandwich panelss," *Construction and Building Materials*, vol. 22, pp. 1009–1018, 2008. [Online]. Available: https://doi.org/10.1016/j.conbuildmat.2007.03.023.

[9] T. Sharaf, W. Shawkat, and A. Fam, "Structural performance of sandwich wall panels with different foam core densities in one-way bending," *journal of Composite Structures*, 2010. [Online]. Available: https://doi.org/10.1177/0021998310369577.

[10] A. Manalo, T. Aravinthan, A. Fam, and B. Benmokrane, "State-of the-art review on frp sandwich systems for lightweight civil infrastructure," *journal of Composites for Construction*, vol. 21, 2017. [Online]. Available: https://ascelibrary.org/doi/10.1061/%28ASCE%29CC.1943-5614.0000729.

[11] O. F. Andrzej, K.BledzkiacHansa, P. Fink, and M. Saind, "Bio-composites reinforced with natural fibers: 2000–2010," *progress in polymer science*, 2012. [Online]. Available: https://doi.org/10.1016/j.progpolymsci.2012.04.003.

[12] L. Wroblewski, D. Hristozov, and P. Sadeghian, "Durability of bond between concrete beams and frp composites made of flax and glass fibers," *Construction and Building materials*, pp. 800–811, 2016. [Online]. Available: https://doi.org/10.1016/j.conbuildmat.2016.09.095.

[13] A. K. Mohanty, M. Misra, and L. T. Drzal, "Sustainable bio-composites from renewable resources : Opportunities and challeneges in the green materials world," *Journal of Postsecondary Education and Disabiity*, vol. 10, pp. 19–26, 1 2002. [Online]. Available: https://link.springer.com/article/10.1023/A:1021013921916.

[14] C. McSwiggan and A. Fam, "Bio-based resins for flexural strengthening of reinforced concrete beams with frp sheets," *Construction and building materials*, vol. 131, pp. 618–629, 2017. [Online]. Available: https://doi.org/10.1016/j.conbuildmat.2016.11.110.

[15] C. Wang, H. H. Khodaparast, M. I. Friswell, and A. D. Shaw, "An equivalent model of corrugated panels with axial and bending coupling," *Computers structures*, vol. 183, pp. 61–72, 2017. [Online]. Available: https://doi.org/10.1016/j.compstruc.2017.01.008.

[16] A. Elmarakbi, *Advanced Composite Materials for Automotive Applications*.

[17] H. Dalir, *Composite for automotive applications*.

[18] Y. Xia, M. Friswell, and E. S. Flores, "Equivalent models of corrugated panels," *International journal of Solids and Structures*, 2012.

[19] *Understanding corrugated material strength ratings : Burst strength vs edge crush testing*. [Online]. Available: https://blog.pantero.com/understanding-corrugated-material-strength-ratings-burst-strength-vs.-edge-crush-testing.

[20] R. Popil, "Overview of recent studies at ipst on corrugated board edge compression strength: Testing methods and effects of interflute buckling," *Bioresources*, vol. 7, 2012. [Online]. Available: doi:10.15376/biores.7.2.2553-2581.

[21] Tomas Nordstrand, "Basic testing and strength design of corrugated board and containers," Doctoralthesis, Lund University, 2003.

[22] *Flexural or bend testing*. [Online]. Available: https://www.touchstonetesting.com/services/material-testing/mechanical-testing/flexural-or-bend-testing/.

[23] P. Sadeghian, "Corrugated cardboard core sandwich beams with bio-based flax fiber composite skins," *journal of Building Engineering*, vol. 20, pp. 114–122, 2018. DOI: https://doi.org/10.1016/j.jobe.2018.07.009.

[24] *Paper and paperboard packaging environmental council*, 2017. [Online]. Available: http://www.ppec-paper.com/pdffiles/factsheets/2017/packaging/fs03-2017.pdf.